

# Deformation of the Dachstein Limestone in the Dachstein thrust sheet (Eastern Alps, Austria)

Oscar Fernandez<sup>1\*</sup>, Bernhard Grasemann<sup>2</sup>, Diethard Sanders<sup>3</sup>

<sup>1)</sup> Dept. of Geology, Univ. of Vienna, Josef-Houlabek Platz 2, 1090 Vienna, Austria

<sup>2)</sup> Dept. of Geology, Univ. of Vienna, Josef-Houlabek Platz 2, 1090 Vienna, Austria

<sup>3)</sup> Dept. of Geology, Univ. of Innsbruck, Innrain 52, 6020 Innsbruck, Austria

\* Corresponding author, oscar.fernandez.bellon@univie.ac.at



## KEYWORDS

Dachstein Limestone, soft-sediment deformation, tectonic deformation, salt tectonics, Eo-Alpine, virtual outcrops

## Abstract

Deformation affecting the Upper Triassic Dachstein Limestone has been analyzed in the Dachstein thrust sheet, the uppermost thrust unit of the central Northern Calcareous Alps (Eastern Alps). Different scales of deformation are discussed, from kilometer-scale thrusting down to folds in the order of tens of meters to meters. Observations are based on both conventional outcrop observations and on digital fieldwork performed on drone-captured virtual outcrops and on GoogleMaps 3D terrain renderizations. The structures observed were formed at different times and document the following events: 1) Late Triassic syn-depositional instability and slumping; 2) Late Triassic syn-depositional growth of the Hallstatt diapir; 3) Late Triassic syn-depositional, salt-driven, extensional faulting; 4) Jurassic-age re-activation of extensional faults; 5) (presumably) Early Cretaceous shortening in both east-west and north-south directions; and 6) (presumably) Late Cretaceous extensional re-activation of faults. The structures and their origin have a bearing on the interpretation of the tectonic evolution of the Dachstein thrust sheet, highlighting the potential relevance of salt tectonics in controlling its structure.

## 1. Introduction

The Middle and Upper Triassic shallow water limestones and dolomites of the Northern Calcareous Alps (NCA), in the Eastern Alps (Fig. 1), are a major relief-forming unit. These carbonates form a 2000 - 3000m thick package and are the thickest units within the carbonate-dominated Triassic to Jurassic stratigraphy of the NCA (Fig. 2). At present these units in the NCA are the main component of the NCA imbricate thrust sheets, detached from their basement along Lower Triassic evaporites (Figs 1 and 2). Despite their thrust imbrication, in the central NCA the Triassic platform carbonates occur as gently dipping slabs of thick carbonate that conform most of the major mountainous massifs of the central NCA (e.g., Fig. 3).

Due to the thickness and lateral continuity of the Middle to Upper Triassic carbonates, geological maps of the area are dominated by large swathes of these units, that present remarkable homogeneity in map view. One of the areas in which this can be clearly seen is in the area along the Traun valley Hallstättersee (Upper Austria, Austria). The geological map of this region (Fig.

3) is dominated by the outcrop of Triassic shallow water limestones; namely Late Triassic Dachstein Limestone, along with its time equivalent Hauptdolomit, and the underlying Middle Triassic Wetterstein Dolomite (Fig. 2). The apparent homogeneity of Triassic shallow water carbonate outcrop is however misleading. On the one hand, the area is cross-cut by a major thrust that forms the base of the Dachstein thrust sheet (Figs 4 and 5). On the other hand, multiple authors have previously documented small-scale deformation such as folding in the Dachstein Limestone (e.g., Spengler, 1918; Medwenitsch and Schauburger, 1951; Schmid, 2009; Fernandez et al., 2021) at a scale that is mostly below the resolution of the 1:50,000 scale maps of the area (those of Plöching, 1982; and Schäffer, 1982). Folding in this area has been documented by the above authors to have different origins.

This paper will review the evidence for folding of the Dachstein limestone in the Dachstein thrust sheet along the Traun River valley (Fig. 4) at sub-kilometer scale, and

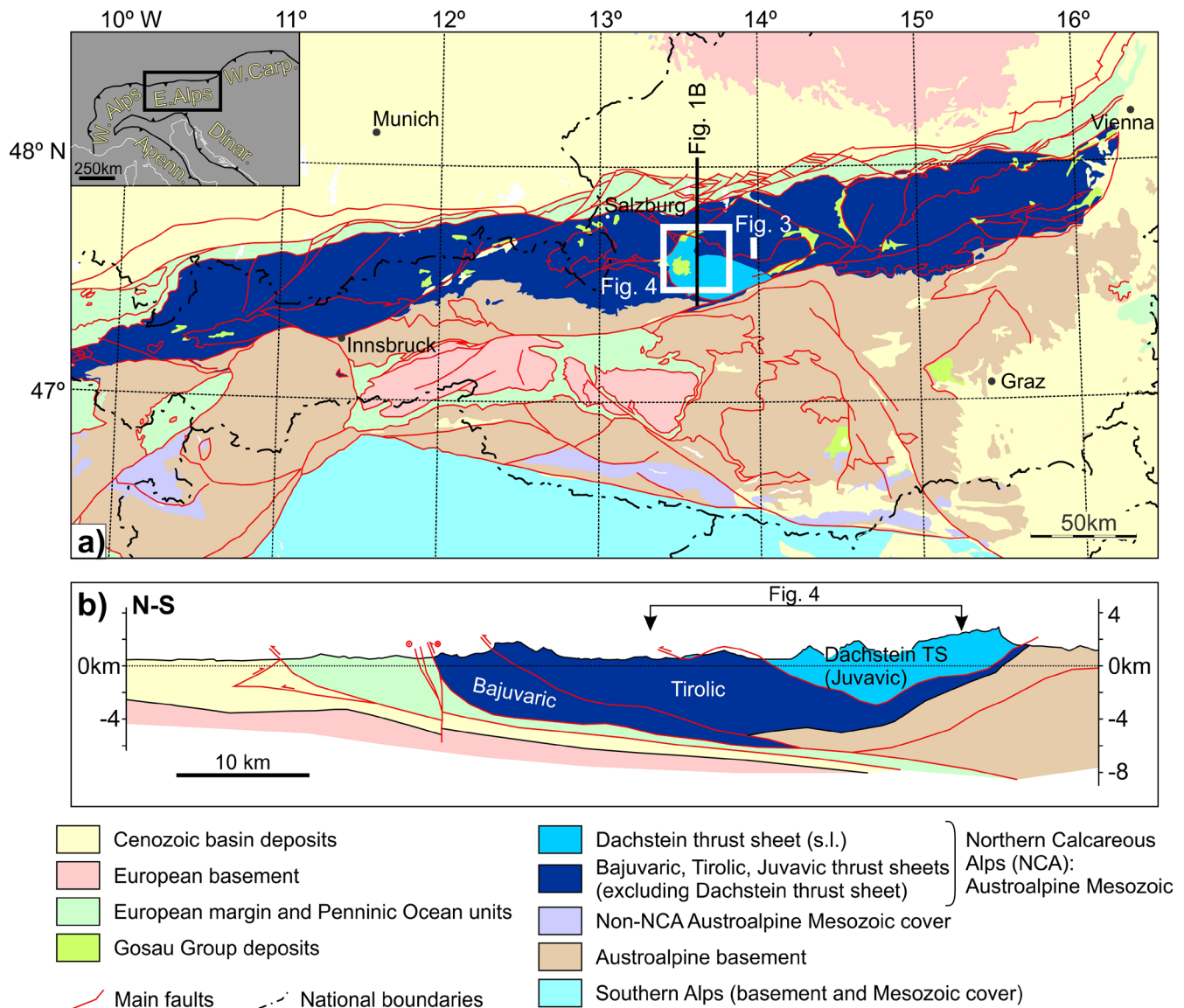


**Figure 1:** (a) Simplified geological map of the Eastern Alps (modified from Schuster et al., 2013 and using the definition of the Dachstein thrust sheet of Tollmann, 1985). See inset for location. The location of the panorama in Figure 2 and the map in Figure 3 are shown. Abbreviations: Apenn. = Apennines, Dinar. = Dinarides, E. = East, W. = West. (b) Simplified cross-section across the northern Eastern Alps (modified from Krenmayr and Schnabel, 2006). The Northern Calcareous Alps (NCA) are an imbricate of 3 main thrust sheets (or sets of thrust sheets) called, from lower to upper, Bajuvaric, Tirolic and Juvavic thrust sheets (TS). This article deals with the Dachstein TS, one of the Juvavic thrust sheets.

discuss its possible origin, as either pre-Alpine (syn-sedimentary or early burial) or Alpine folding. Beyond what is immediately visible in outcrop, or what can be captured in drone-derived virtual outcrops, the openly available, 3D rendered terrain models generated by GoogleMaps (maps.google.com) make it possible to view this region with oblique aerial views and explore sectors that have been to date difficult to reach. In this sense, this paper in part also intends to act as an example to extend the existing field database with virtual outcrops in future investigations.

## 2. Background

The NCA is a roughly E-W trending imbricate system of thrust sheets involving rocks of dominantly Triassic to

Jurassic age. The Triassic to Jurassic sediments forming the NCA were initially deposited on the Alpine-Carpathian-Pannonian block (ALCAPA of Schmid et al., 2008) before being mostly decoupled from their underlying crystalline basement and being thrust over the Penninic Ocean and the southern margin of the European continent during Alpine orogenesis (Froitzheim et al., 2008; Schmid et al., 2008). Thrust sheets in the NCA are conventionally grouped into three systems, that from structurally lowest to highest are the Bajuvaric, Tirolic and Juvavic systems (Fig. 1b). The area of study lies in the Juvavic unit of the central NCA, where this unit is formed solely by the Dachstein thrust sheet (TS) (Dachstein nappe of Mandl, 2000; Figs 1 and 4). Units that have traditionally been considered to be a structurally lower nappe (i.e., Lower

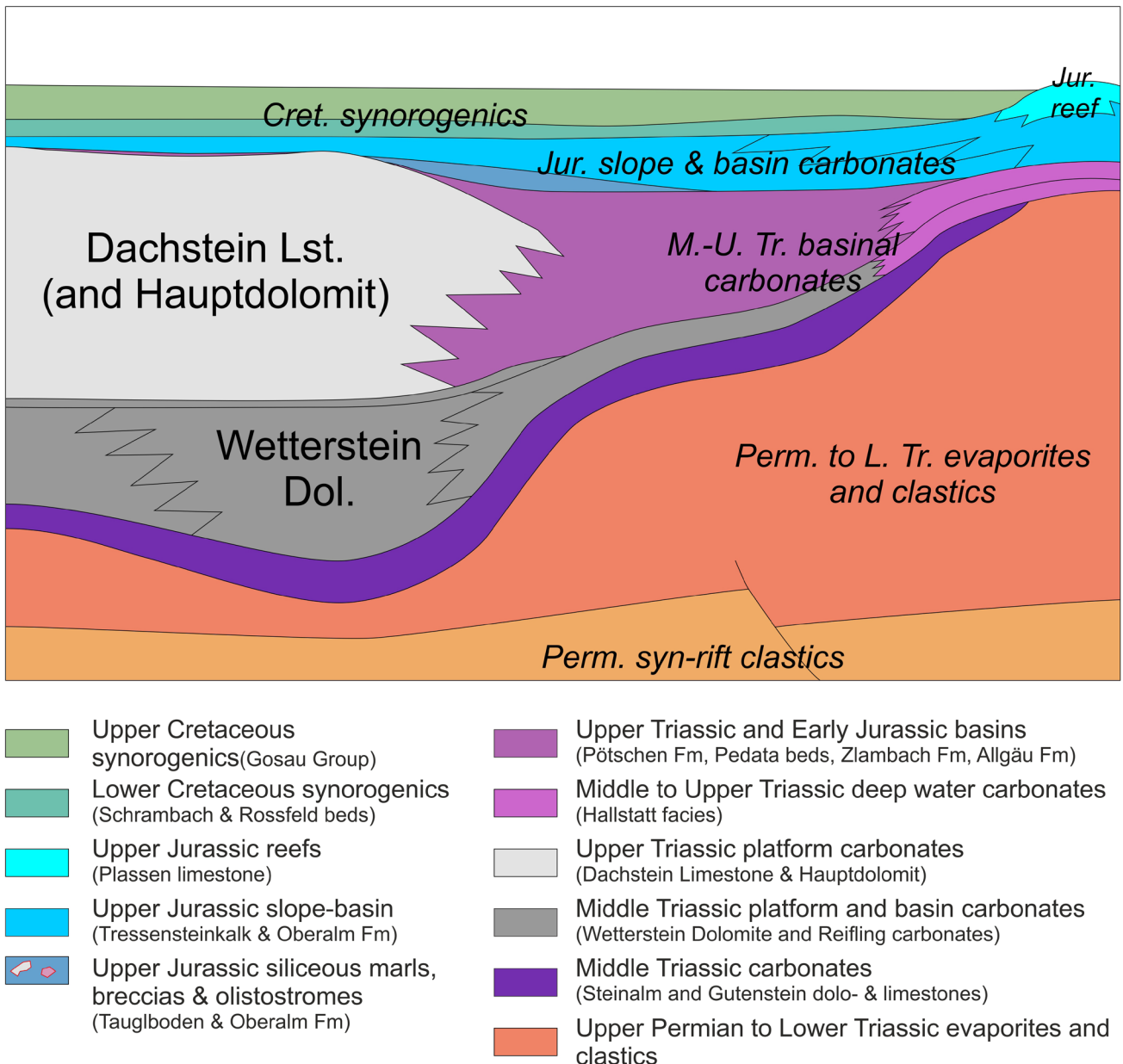


**Figure 2:** Simplified stratigraphic scheme of the central NCA. Triassic deposition was strongly controlled by syn-sedimentary salt tectonics that controlled the distribution of carbonate facies. The Dachstein Limestone, subject of this study, was deposited in a platform setting and aggraded locally to over 1500 m thickness. Expanded and modified from Mandl (2000). Abbreviations: Cret. = Cretaceous, Dol. = Dolomite, L. = Lower, Lst. = Limestone, Jur. = Jurassic, M. = Middle, Perm. = Permian, Tr. = Triassic, U. = Upper.

Juvavic unit) are interpreted to be part of either the Juvavic or Tirolic units based on their position (Mandl, 2000; Fernandez et al., 2021; Fernandez et al., 2022).

During the Triassic, prior to the Jurassic opening of the Penninic Ocean, the ALCAPA block still constituted the southern-facing passive margin of the European continent. During this time, sedimentation on this margin evolved from epicontinental settings during the Late Permian and Early Triassic, which led to the widespread deposition of evaporites (Late Permian Haselgebirge Fm; Leitner et al., 2017) and continental clastics, to marine settings dominated by carbonate sedimentation from

the Middle Triassic through to the Late Jurassic (Fig. 2; Tollmann, 1976; Mandl, 2000 and references therein).

Within this Triassic to Jurassic carbonate succession, this article focuses on the Late Triassic Dachstein Limestone, which is described here based on the syntheses of Tollmann (1976) and Mandl (2000). This unit is an 800-1500 m thick shallow water carbonate succession that can be encountered along the southern margin of the NCA, east of the locality of Lofer (Salzburg). This unit is characterized by deposition in either a back-reef lagoon setting or in reef buildups along the platform margin or in intra-lagoonal settings. The reefal Dachstein Limestone

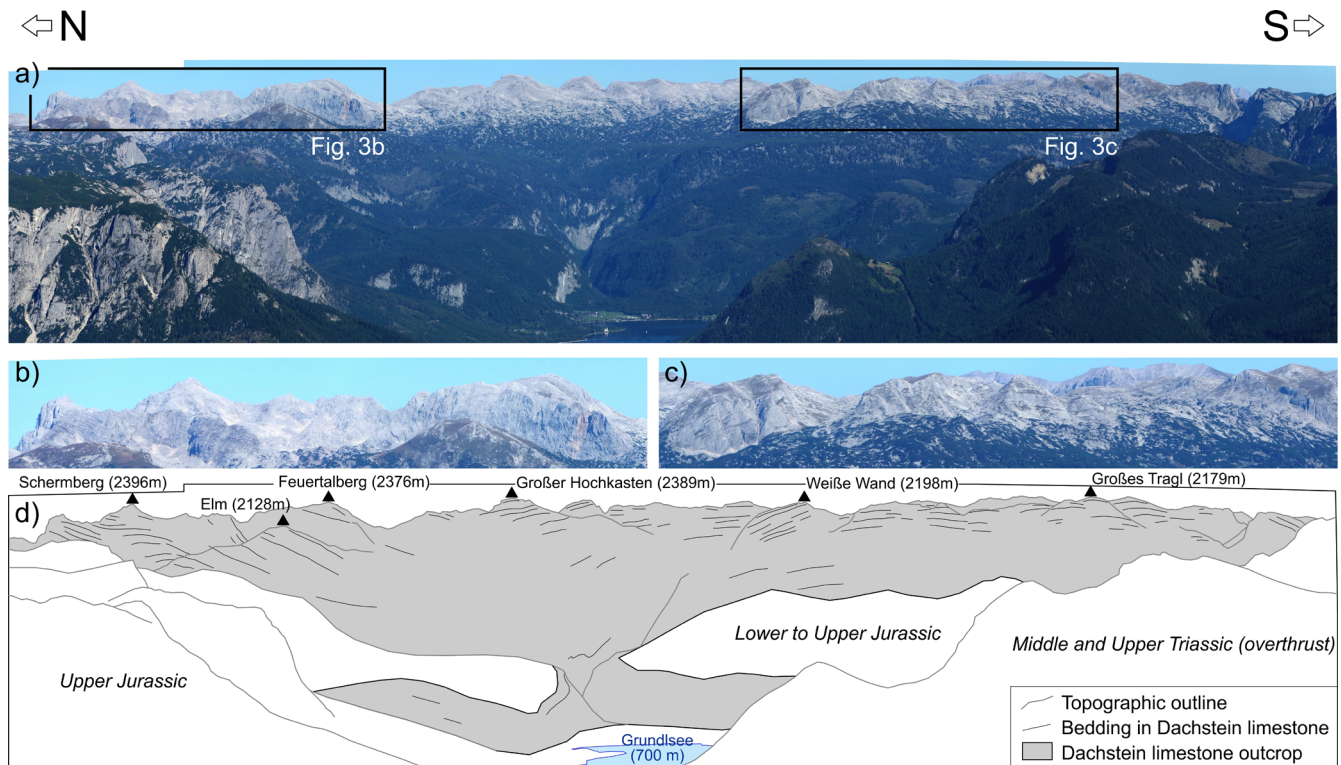


**Figure 3:** Westward looking panorama view of the Totes Gebirge massif in Upper Austria (taken from the Hoher Sarstein to the east). The uninterpreted panorama is shown in (a), details are shown in (b) and (c), and the interpretation in (d). The panorama is roughly N-S oriented and shows the massif is made up of mostly gently dipping and gently folded Late Triassic Dachstein Limestone. Only locally (between the Schermberg and Feuertalberg) do beds dip over 30°, and still then, folding is gentle. The foreground is dominated by Jurassic sediments that lie on and overlap the Triassic Dachstein Limestone, which dips subhorizontal or gently westward under the Jurassic. The ridge crossing down from the south of the image is made up of thrustured Triassic carbonates (including the Dachstein Limestone). The image is roughly 13 km across in the background. See Figure 1 for approximate location.

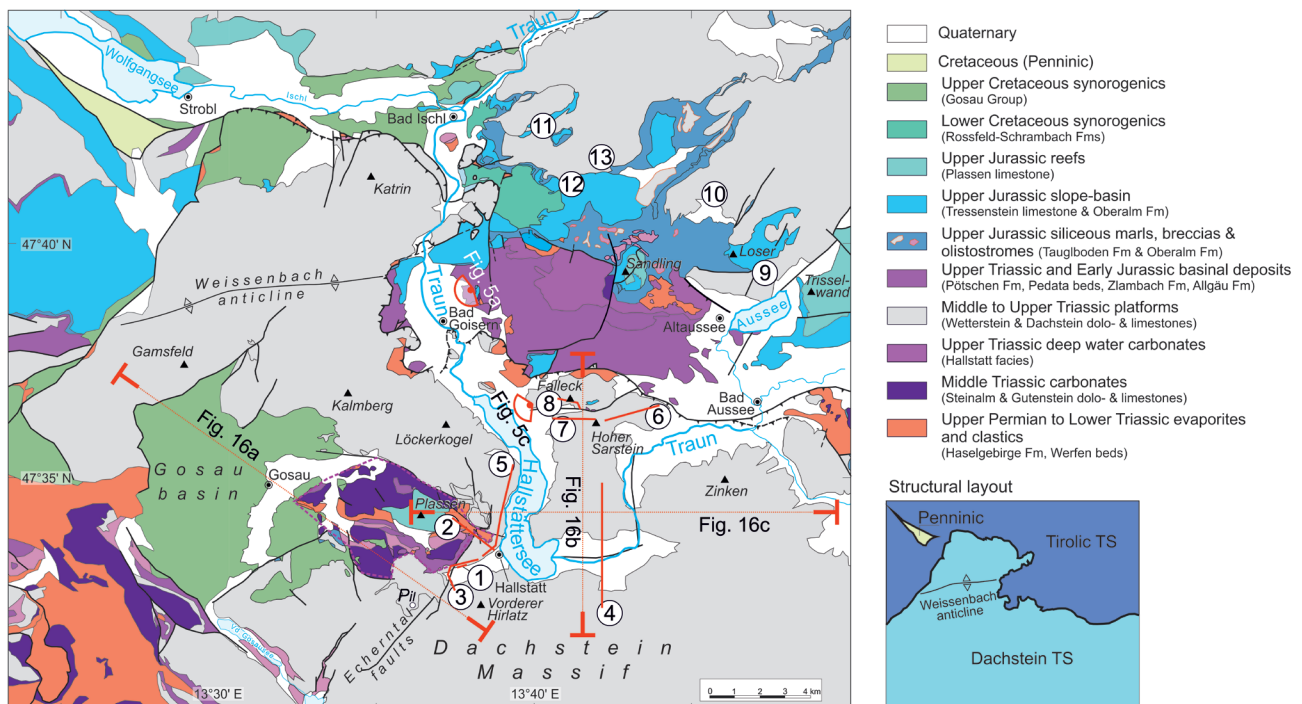


**Figure 4:** Simplified geological map of the study area. Number labels refer to the outcrops discussed in this article: 1 = Fig. 6; 2 = Fig. 7; 3 = Fig. 8; 4 = Fig. 10a; 5 = Fig. 11; 6 and 7 = Fig. 12; 8 = Fig. 13; 9 = Fig. 14; 10 - 13 = Fig. 15. The approximate outline of the Hallstatt diapir is shown by the dashed magenta line NE of the village of Hallstatt. Location of the sample discussed in section 4.3 (west of the Echerntal faults) is marked by the label P<sub>11</sub>. See Figure 1 for location. Modified from Mandl et al. (2012), Plöching (1982), Schäffer (1982). Abbreviation: TS = thrust sheet/system.

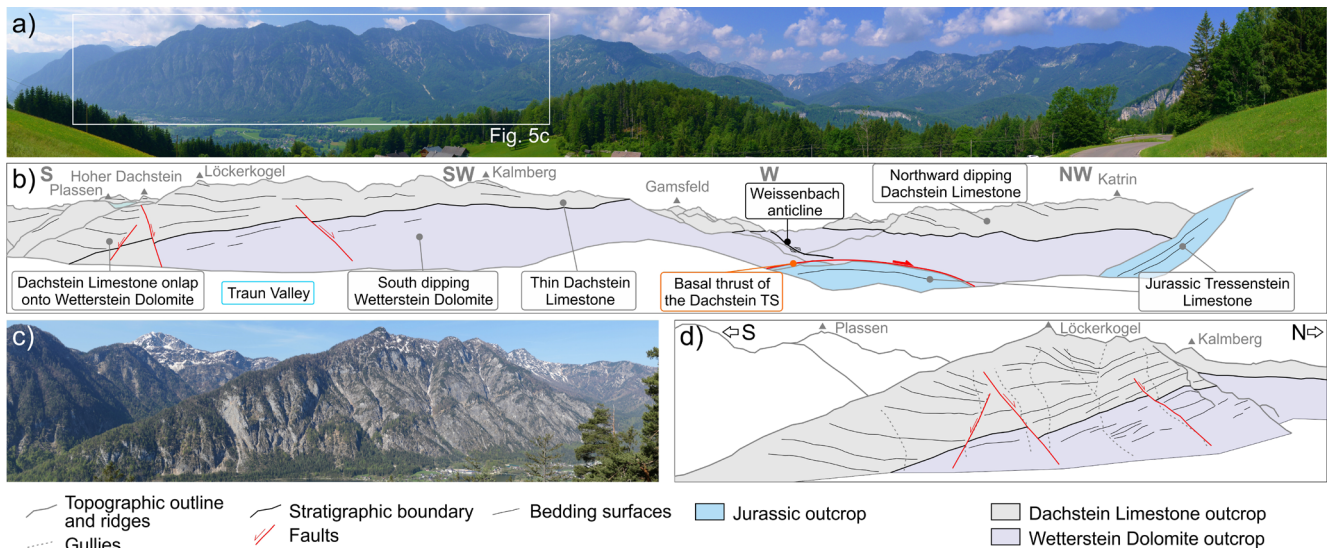


**Figure 5:** Panorama of the Dachstein thrust sheet west of the Traun Valley (a) and interpretation (b). Note that the thrust sheet outcrop is dominated by the Middle to Late Triassic Wetterstein Dolomite and Dachstein Limestone, which locally reach a thickness of over 2000 m. Despite the thrust having a displacement of at least 10 km, the Triassic carbonates are only gently folded into a broad anticline (Weissenbach anticline of Tollmann, 1985). On the southern limb of the anticline (detailed panorama from the West shown in c, d) the Wetterstein Dolomite can be recognized to dip to the south whereas the Dachstein Limestone dips gently or even to the north and onlaps onto the contact with the Wetterstein Dolomite. The result is a northward thinning of the Dachstein Limestone that can be recognized north of the Kalmburg. For the location of the viewpoint for the panoramas in (a) and (c), see Figure 4.

is massive and bedding is largely absent. In contrast, the lagoonal facies of the Dachstein Limestone are well bedded and present carbonate beds that are tens of centimeters to a few meters thick, due to their deposition in eustatically controlled cycles known as the Lofer cyclothems (Fischer, 1964).

This well-bedded Dachstein Limestone is dominant in the Dachstein TS, forming most of the outcrop along the southern portion of the Traun River valley and the Hallstättersee (Fig. 4). This dominance is only interrupted east of the village of Hallstatt by a patchy arrangement of condensed shallow and deeper water Triassic carbonates, as well as outcrops of Jurassic carbonates and Cretaceous Gosau Group sediments that overlie the Hallstatt diapir (Fig. 4). This area has also been previously documented to host Dachstein Limestone that locally deviates from the gently dipping and gently folded structures observed more regionally (e.g., Fig. 3). Already Spengler (1918) and Medwenitsch and Schauburger (1951) documented in their profiles that the Dachstein Limestone in the vicinity of the Hallstatt diapir is folded at sub-kilometer scale and even, locally, vertically dipping. More recently, folding has been the subject of the detailed study of Habermüller (2005) and Schmid (2009) who attempted to account for the origin of folds in the scale of tens to hundreds of meters. Some of the structures initially documented by Medwenitsch and Schauburger (1951), Habermüller (2005) and Schmid (2009) were later reinterpreted by Fernandez et al. (2021) as relating to folding in the Dachstein Limestone during growth of the adjacent Hallstatt diapir. Inherent to the concept of syn-diapir folding is the fact that some of these folds have formed during deposition or in early

burial, and therefore are not related to Eo-Alpine or Alpine tectonics.

### 3. Folding and deformation in the Dachstein Limestone

This section contains a description of observed fold and other “anomalous” geometries and their interpretation based on our current understanding of the area. Based on their origin, the structures can be classified as syn-depositional (when there is evidence of intra-formational unconformities sealing deformation or thickening or thinning of beds due to structure development) or as tectonic (when there is absence of these criteria) (Ortner, 2007; Alsop et al., 2019). Furthermore, since limestones can only fold ductily by dissolution-precipitation processes, tectonic folds should record, in fold hinge areas, structures like dissolution seams, stylolites or calcite precipitation in veins. In fault-related folds that were formed in lithified rock during tectonic shortening, and not in unconsolidated sediments during slumping, folds should record evidence of flexural slip and faults should contain evidence for fault rocks formed through brittle deformation.

We have further subdivided tectonic structures into two groups based on their scale: those structures that involve all or most of the Dachstein Limestone as a coherent unit (large-scale structures), and those that use intra-formational detachments and therefore generate folds of a smaller amplitude (small-scale structures).

#### 3.1 A note on the source of imagery

The observations presented below are based on three different data sources. Firstly, there are conventional

field observations and photographs. Some of the best outcrops for structural observations in the Dachstein Limestone are vertical walls tens to hundreds of meters high, providing excellent exposure. However, precisely because of the steepness and dimensions of the outcrops, it is not always possible to obtain good vantage points in the field. Therefore, two additional data sources have been used. One is 3D digital outcrop models generated from images captured with a DJI Mavic 2 drone using a Structure from Motion algorithm implemented in Agisoft Metashape Professional 1.8.2 ([www.agisoft.com](http://www.agisoft.com)). These models can be manipulated in technical software, and can, amongst other things, be analyzed to extract dip measurements of features inaccessible in the field. The second additional source of imagery is the 3D renderization of topography provided in GoogleMaps ([maps.google.com](http://maps.google.com)). This renderization has been recently updated in part of Upper Austria (first noticed by the authors in 2021) and appears to be the result of applying Structure from Motion to aerial or satellite photography. This novel renderization has a highly improved resolution in terms of the terrain model and provides exceptional views of vertical or steep wall outcrops that would be impossible with traditional draping of imagery on digital terrain models.

### 3.2 Syn-depositional structures

Documenting syn-depositional structures is difficult due to the imperative of encountering unambiguous indicators of the progression of deformation during deposition. In this sense, however, the outcrop of the Echernwand, just east of the village of Hallstatt (number 1 in Fig. 4; Fig. 6a), discussed by Fernandez et al. (2021) presents an outstanding example. This outcrop reveals the vertical stacking of sequences of Dachstein Limestone beds, folded and bounded by unconformities. These beds were deposited, deformed and truncated during growth of an adjacent salt structure and can therefore be considered halokinetic sequences (*sensu* Giles and Rowan, 2012). The salt body against which these sequences developed, most likely a branch of the Hallstatt diapir, has since been squeezed out during Alpine shortening and all that remains is a weld juxtaposing rocks that were at one point on opposite sides of the salt body. The fact that the Dachstein Limestone west of the weld does not present halokinetic sequences equivalent to that on the east indicates that some amount of strike-slip displacement must have taken place, and the opposite side of the salt body has been offset due to this motion. Alternatively, one would expect beds on both sides of the weld to have a similar structure (e.g., Giles and Rowan, 2012). This weld, which is complete (i.e., no remaining evaporites within the weld) at the outcrop location of the Echernwand, is also found within the Hallstatt mine Erbstollen (base gallery) and was documented by Medwenitsch and Schauburger (1951) where shales of the Permian age Haselgebirge Fm are still present between two walls of Dachstein Limestone (Fig. 7).

The outcrop and overall setting of the halokinetic sequences has been presented by Fernandez et al. (2021). In this section we will concentrate on the lowermost two sequences as seen in Figure 6a. The two sequences are adjacent to the sheared weld, a major sub-vertical feature (dipping  $\sim 250/65$ ) that runs the height of the outcrop (label 1 in Fig. 6b) and can be followed in the forest above the outcrop. The two halokinetic sequences in Figure 6a are separated by an angular unconformity (label 3 in Fig. 6b). The beds in the lower sequence (sequence 1, Fig. 6b) are folded into an east-verging syncline. Towards the base of this sequence (interval 1.1, Fig. 6b), beds are mostly parallel to each other and onlap onto the weld (label 1, Fig. 6b). Towards the top of sequence 1, angularities and thickness changes (interval 1.2, label 2, Fig. 6b) record some degree of deformation in the vicinity of the salt body. The overlying sequence (sequence 2, Fig. 6b) presents a similar pattern of beds onlapping onto the weld (albeit in the opposite direction; interval 2.1, label 4, Fig. 6b) but being roughly parallel to each other. Towards the top of sequence 2 (interval 2.2, label 5, Fig. 6b) internal onlap towards the west is also seen.

The outcrop in Figure 6a also shows the presence of small scale shortening structures (label 7 in Fig. 5b) that post-date the development of the halokinetic sequences and are most likely of Alpine or Eo-Alpine age (as those documented by Schmid, 2009). This event of shortening is likely in part responsible for the welding of the salt body and shearing of the weld contact.

Finally, the outcrop in Figure 6a also shows the presence of extensional, syn-depositional faults (label 6 in Fig. 6b) that are part of a set of faults striking northeast-southwest across the Echerntal Valley, roughly parallel to the weld of Figure 6. This system of faults (called here the Echerntal faults, label 1 in Fig. 8) dips to the northwest and prolongs to the southwest (label 2 in Fig. 8; see also Fig. 13). The faults cause down-throw of the northwestern block and thickening of the Dachstein Limestone towards the west and southwest (labels 3, Fig. 8) due to syn-depositional activity. Due to outcrop constraints (most of the Dachstein Limestone in the hanging wall of the Echerntal faults lies underground), growth geometries can only be ascertained in the uppermost few hundred meters Dachstein Limestone (labels 3, Fig. 8; note that the top of the Triassic is marked by Jurassic sediments directly overlying the Dachstein Limestone: label 4, Fig. 8).

### 3.3 Large scale structures

A very remarkable feature affecting the Dachstein thrust sheet is the presence of a significant drop in the elevation of the top of the Dachstein Limestone north of the Dachstein Massif. This drop can be observed both to the west and the east of the Hallstättersee. West of the Hallstättersee, the drop occurs in the Echerntal Valley across the SW-NE trending Echerntal faults (Fig. 8, label 1 in Fig. 9c). These faults and the accompanying drop in the Dachstein are reflected in the topography to the southeast of the Echerntal Valley (Fig. 9a-b, label 2 in

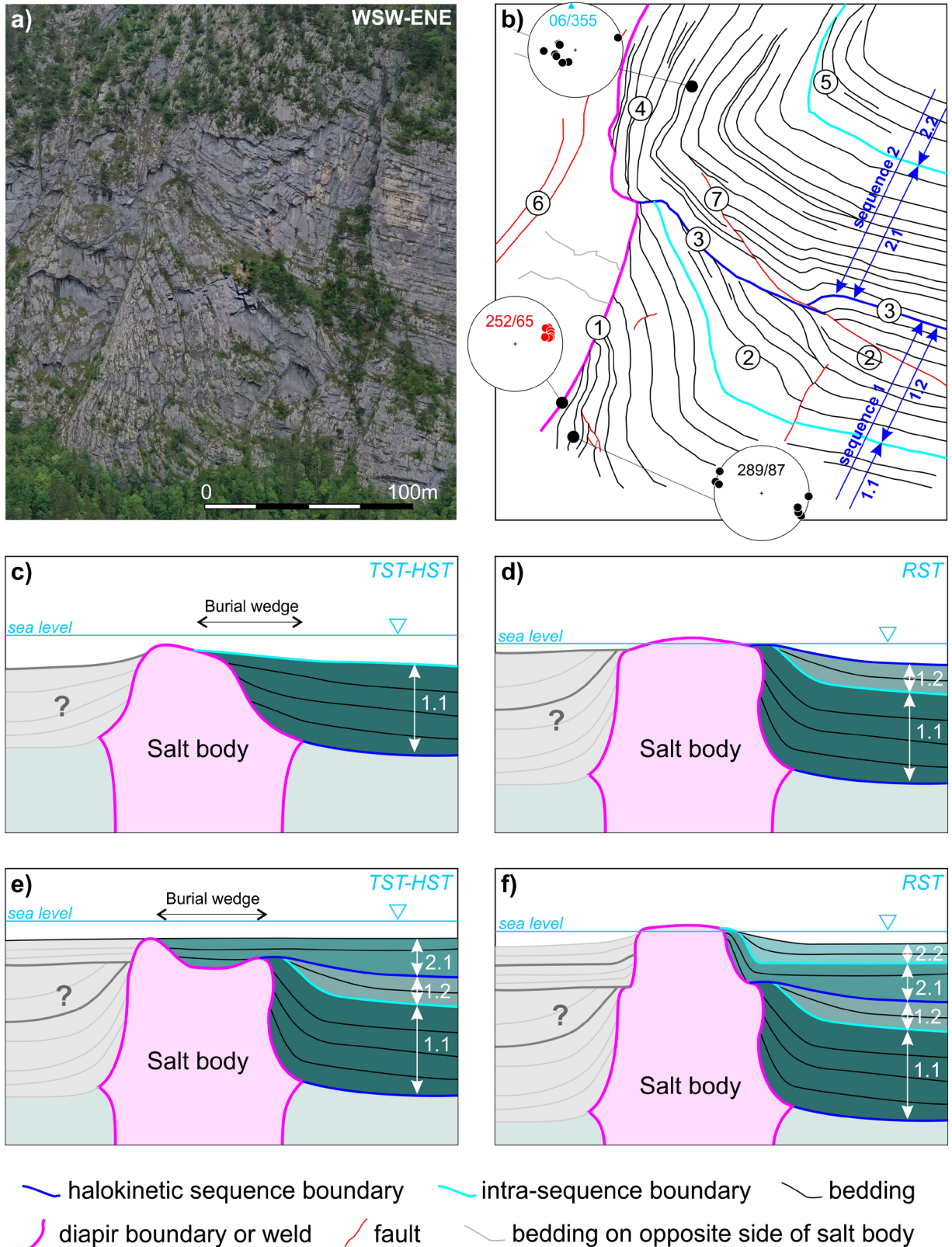


**Figure 6:** (a) Orthophotograph extracted from a 3D outcrop model (Fernandez et al., 2021) of a sheared secondary weld in the Echernwand, some 2 km east of the village of Hallstatt. Outcrop is labelled 1 in Figure 4. (b) Line interpretation of the image in (a). Stereoplots show bedding (black) and sheared weld (red) dip measurements extracted from the 3D outcrop model of Fernandez et al. (2021) and obtained in the field. Values in the stereoplots (equal area, lower hemisphere) represent average orientation (red and black) and fold axis (blue). 1 = Sheared salt weld; 2 = thickness changes in interval 1.2; 3 = sequence boundary; 4 = east-directed onlap onto salt weld; 5 = thickness changes in interval 2.2; 6 = extensional faults of the Echernthal; 7 = west-directed thrust. (c), (d), (e), and (f) show the evolution of the salt body (whose only relic is the weld) based on the geometry of beds interpreted in (b). Abbreviations: HST = highstand system tract, RST = regressive system tract, TST = transgressive system tract.

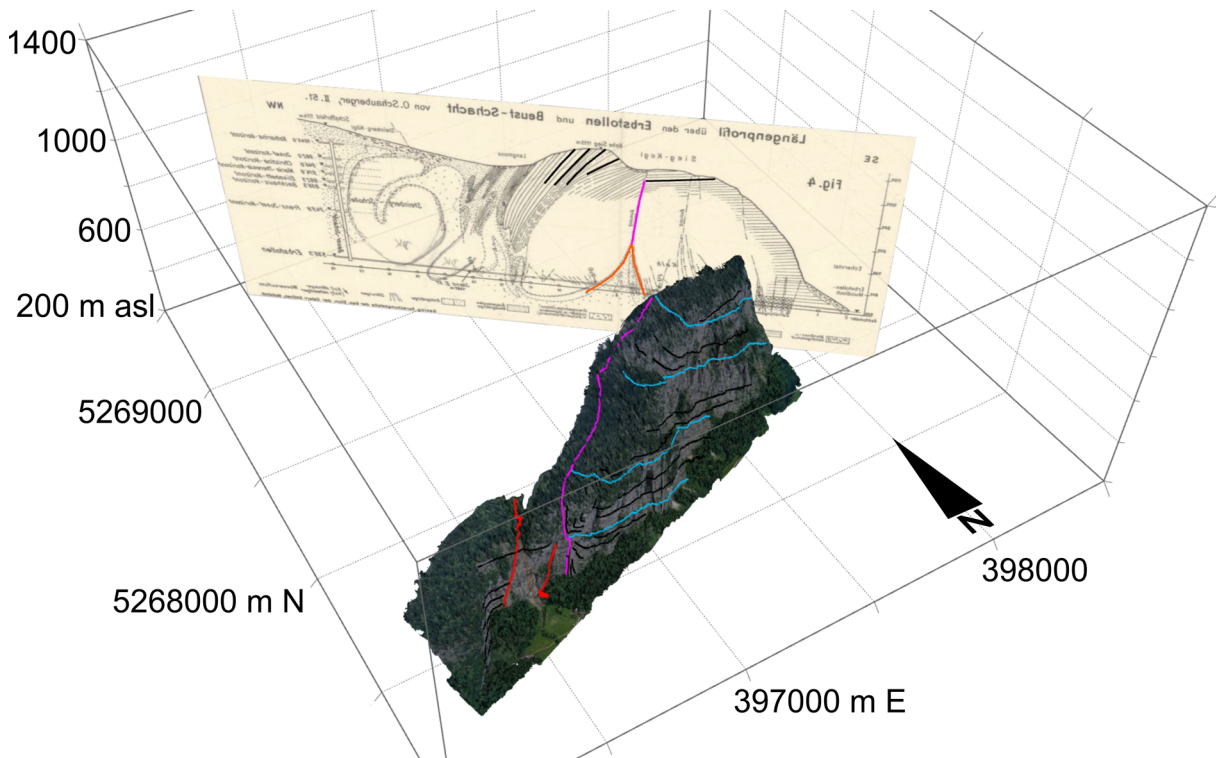


**Figure 7:** Oblique view from the SW of the entire Echernwand outcrop and its interpretation (from Fernandez et al., 2021) with the section of the Hallstatt Erbstollen by Medwenitsch and Schaubeger (1951). The weld on the outcrop is marked in magenta. An equivalent structure along strike has been identified in the Erbstollen gallery, as a wedge of sheared black shales of the Haselgebirge Fm between two walls of Dachstein Limestone (orange wedge structure) and interpreted by Medwenitsch and Schaubeger (1951) to weld upwards (magenta line on the profile). The profile of Medwenitsch and Schaubeger (1951) also contains the observation of vertical to overturned beds and is presented as published, without being revised for consistency with the outcrop structure. The outcrop of the weld is up to 1300 m away from the gallery at its farthest. The location of the profile is labelled 2 in Figure 4. Coordinates are in meters. XY coordinates are in meters and UTM33 WGS84. Vertical scale in meters above sea level.

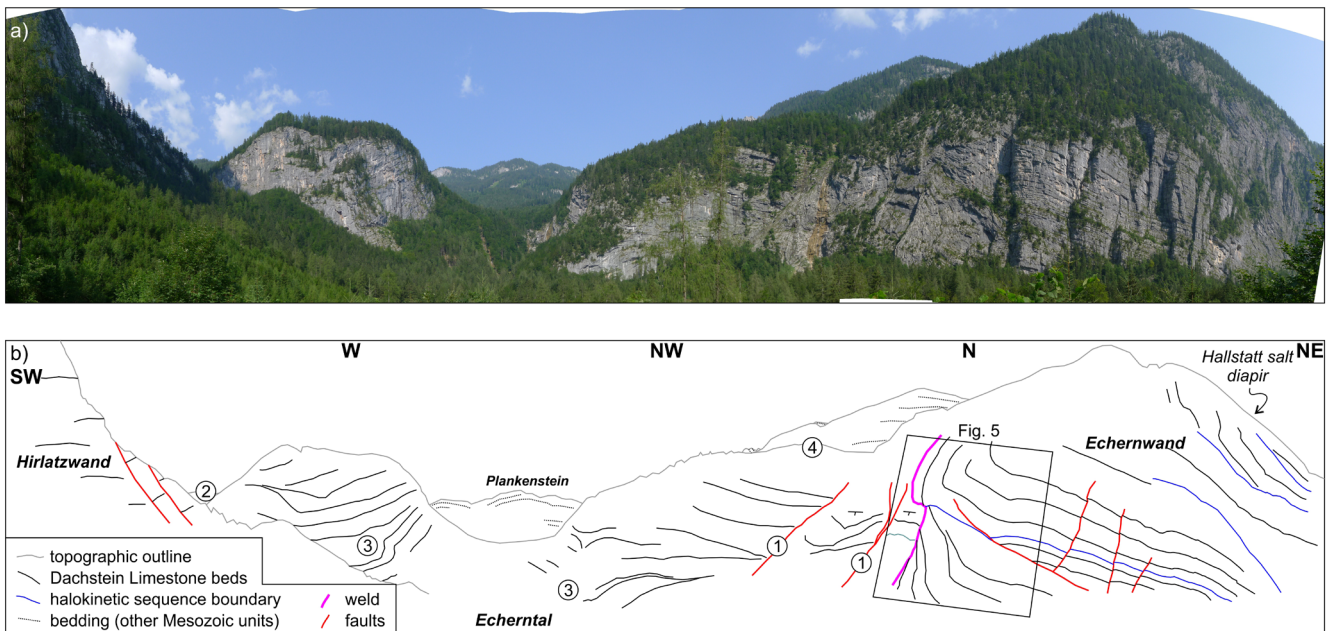


**Figure 8:** Panorama view of the Echerntal Valley, between the Echernwand to the north and the Hirlatzwand to the south (a) and its interpretation (b). 1 and 2 = Echerntal extensional faults and southwestward prolongation; 3 = growth geometries in Dachstein Limestone; 4 = location of the stratigraphic top of the Dachstein Limestone (and presence of Jurassic sediments). The location of the outcrop in Figure 5 is shown. The location of the foreground in this panorama is labelled 3 in Figure 4.

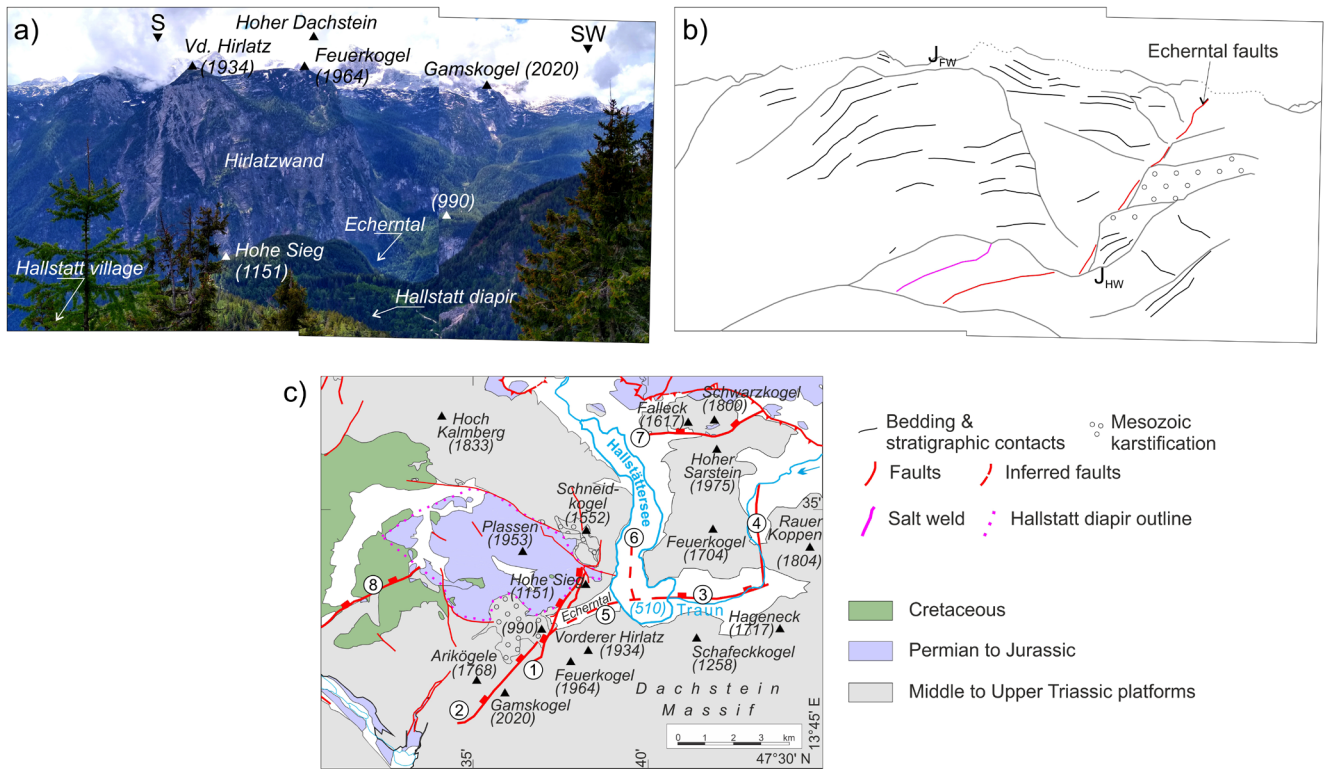


**Figure 9:** (a) Panorama view looking south from the Schneidkogel (see c for location) over the Echerntal and the Hirlatzwand. (b) Line drawing interpretation of (a).  $J_{HW}$  marks the position of the base of the Jurassic north of the Echerntal (in the hanging wall of the Echerntal faults) and  $J_{FW}$  marks the base of the Jurassic above the Hirlatz Wall, in the footwall of the Echerntal faults. (c) Simplified map of the northern Dachstein Massif and location of key faults (modified from Mandl et al., 2012). 1 and 2 = Echerntal faults and southwestern prolongation; 3 = Obertraun fault; 4 = tear fault accommodating Obertraun offset to the west; 5 = eastward prolongation of the Obertraun fault under the Echerntal valley; 6 = fault under the Hallstättersee; 7 = Sarsteinalm fault; 8 = Gosau basin bounding fault. In (a) and (c), elevations in meters above sea level are shown in brackets.

Fig. 9c). Offset on the Echerntal faults also involves the Jurassic, which is downthrown along with the Dachstein Limestone (Fig. 9b).

Offset in the top of the Dachstein is also evident further east in the Echerntal Valley, in the footwall of the Echerntal faults, as can be seen by topography being roughly 800 m lower to the north of the valley (compare Hohe Sieg and Vorderer Hirlatz peaks in Fig. 9a, c). East of the Hallstättersee, the drop in the Dachstein Limestone is even more evident (location of label 3 in Fig. 9c, Fig. 10). At this location, beds in the Dachstein Massif (south of the Traun, label 1 in Fig. 10b) and in the foreground (label 2 in Fig. 10b) dip horizontal or slightly to the north. The top of the Dachstein Limestone in the Massif is not visible in the image and is hundreds of meters higher. On the north of the Traun, the top of the Dachstein Limestone (label 3 in Fig. 10b) is seen to dip southwards into the Traun Valley. A north-dipping, roughly east-west striking normal fault is interpreted to run along the Traun Valley near the vicinity of Obertraun (label 3 in Fig. 9c, label 4 in Fig. 10b). The fault (called here the Obertraun fault) dies out to the west and its roughly 800 m of offset are accommodated to the west by a north-south tear fault (label 4 in Fig. 9c, label 5 in Fig. 10) separating the dipping Dachstein Limestone monocline from the sub-

horizontal Dachstein Limestone in the foreground of Figure 10 (label 2). This tear fault dies out to the north, within the valley. Towards the east, the Obertraun fault likely continues with a roughly E-W trend along the Echerntal valley (label 5 in Fig. 9c) causing the lowering of the footwall of the Echerntal faults (the Hohe Sieg block) discussed above. However, in contrast to the monocline observed in the hanging wall of the Obertraun fault in the Traun valley, the Hohe Sieg block is lowered without being tilted southward. To accommodate the difference in geometry of the hanging wall, a fault is likely also present in the Hallstättersee (label 6 in Fig. 9c), west of the monocline and east of the Hohe Sieg.

This monoclinical structure also involves the underlying Middle Triassic Wetterstein Dolomite (Fig. 10), but unlike the Echerntal faults, it has no related thickness changes in the Dachstein Limestone. There is also no preserved Jurassic or Cretaceous above the Dachstein Limestone at this location (likely eroded glacially), making it difficult to date activity on the extensional fault.

Finally, another E-W trending, northward dipping fault is located north of the Obertraun fault, immediately north of the Hoher Sarstein (label 7 in Fig. 9c). This fault (called here the Sarsteinalm fault) has a smaller offset (under 400 m) than the Obertraun and Echerntal faults.

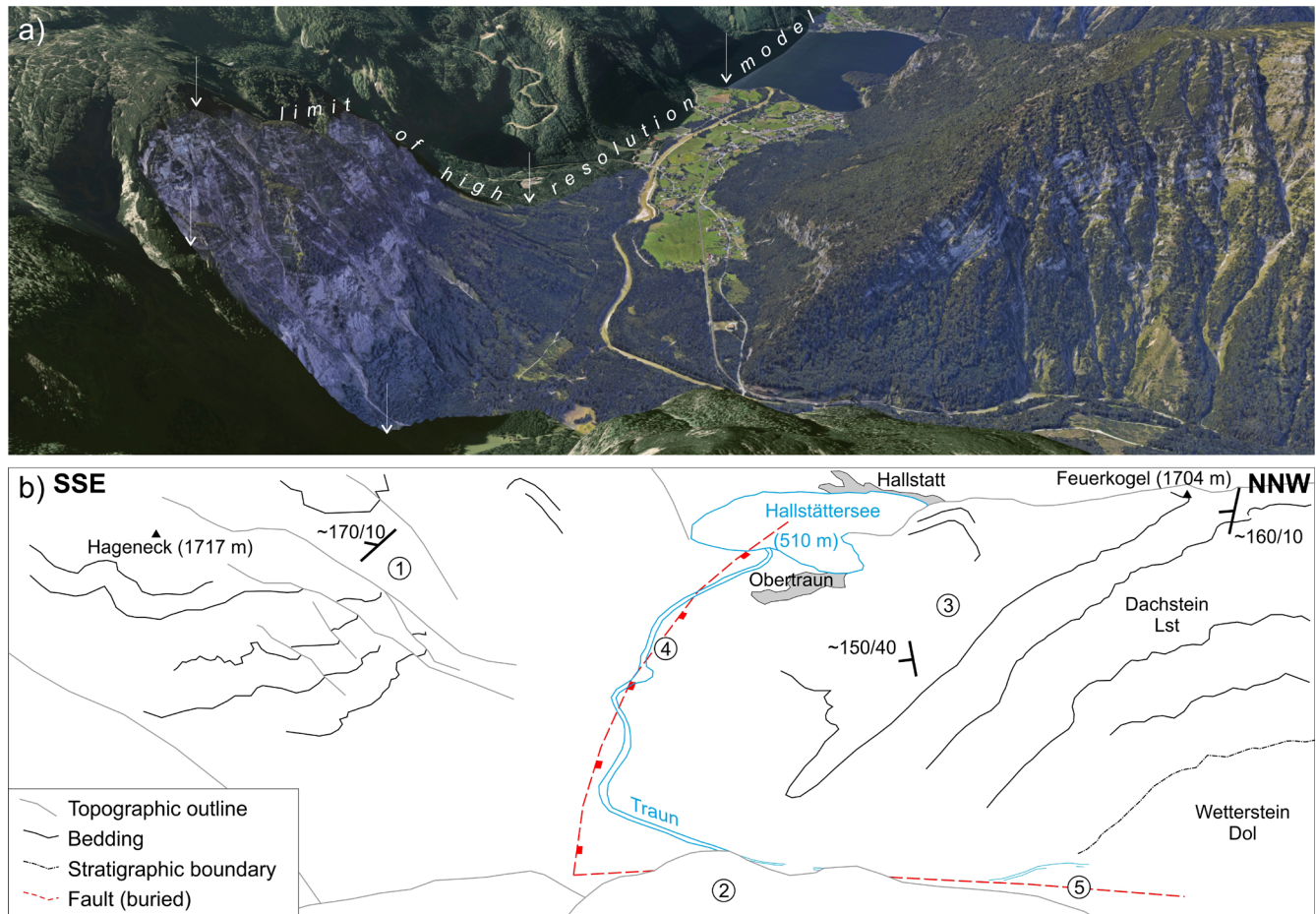


**Figure 10:** (a) West-directed oblique aerial view of the Traun Valley immediately east of Hallstättersee. Image captured in GoogleMaps (captured 25 Jan. 2022; imagery from Geoimage Austria, CNES/Airbus, Maxar Technologies, Salzburg AG/Wenger Oehn). The image is roughly 6 km long and labelled 4 in Figure 4. White arrows indicate a boundary between different resolution imagery and topography (lower resolution to the left). (b) Interpretation of the panorama in (a). The area is dominated by Dachstein Limestone (Lst) outcrop excepting in the bottom right-hand corner where the Wetterstein Dolomite (Dol) crops out. 1 and 2 = Sub-horizontal Dachstein Limestone; 3 = southward dipping top of the Dachstein Limestone; 4 = trace of the buried Obertraun fault.

However, the Dachstein Limestone in the hanging wall of the Sarsteinalm fault is overlain locally by deep water Hallstatt limestones that outcrop against the fault (Schäfer, 1982) (Fig. 13c) and are equivalent in age to the youngest Dachstein Limestone (Mandl, 2003). The presence of Hallstatt facies limestones in the hanging wall of the Sarsteinalm fault indicates that offset on the fault is at least in part of Triassic age, with fault offset providing the bathymetry necessary for the deposition of the deep-water facies. The drowning of the Dachstein platform and onset of (condensed) deep water carbonate deposition in the hanging wall of the Sarsteinalm fault is likely the cause for the change in thickness in the Dachstein Limestone between both fault blocks (around 600 m to the north, and over 900 m to the south).

The Triassic north of the Sarsteinalm fault is in turn overlain by Middle Jurassic radiolarites and by Upper Jurassic reef-slope limestones (Schäfer, 1982; Mandl, 2003; Schlagintweit and Gawlick, 2006). In spite of previous mapping indicating a laterally continuous radiolarite outcrop (Schäfer, 1982; Mandl, 2003) the Jurassic units

onlap onto the Dachstein Limestone northwards, such that in that direction the reef-slope limestones come to overlay the Dachstein Limestone directly, or at most with thin fragments of condensed red limestone (Fig. 13c, d) (Schlagintweit and Gawlick, 2006).

### 3.4 Small scale structures

In contrast to the extension driving the development of the structures of the Traun and Echerntal Valleys, the other large-scale structure observable in this area is related to shortening and is the basal thrust transporting the Dachstein thrust sheet (Fig. 4, Fig. 16b). This structure, however, is not the subject of this article as it is a well-documented feature (e.g., Mandl et al., 2012). Attention in this section will focus on shortening-related structures of a smaller scale, and that do not involve the entire Dachstein Limestone unit. Some of these shortening structures in the vicinity of the Hallstatt diapir were described by Arnberger (2006) and Schmid (2009) and will not be further discussed here. Instead, attention will focus on contractional structures in the sector flanking

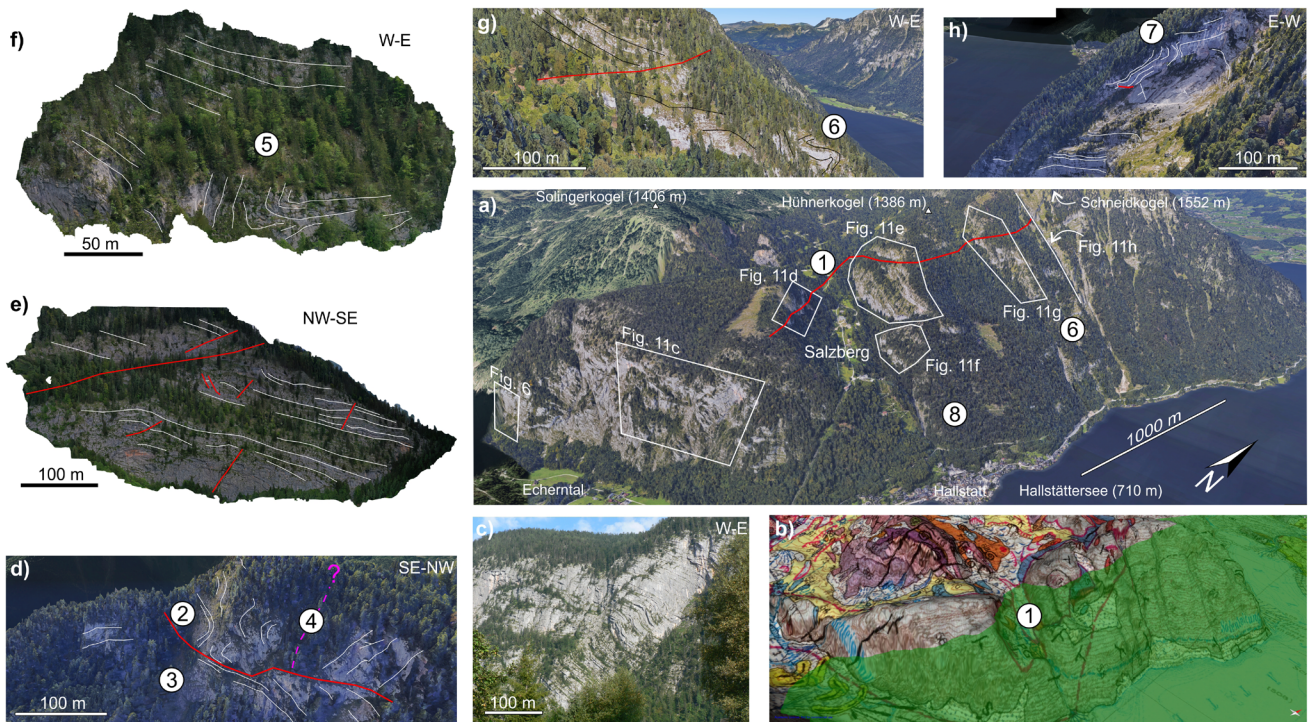


**Figure 11:** (a) - (h) Different views of the Salzberg thrust and related structures arranged clockwise starting from center right. Black and white lines are interpreted bedding, red lines are thrusts and normal faults. Number labels are described in the text. The location of the outcrop in Figure 6 is shown for reference. (a) Oblique aerial view of the western slope of the Hallstättersee (lake is bottom right). The location of this transect is labelled 5 in Figure 3. (b) Oblique view equivalent to (a) with the geology draped on the topographic surface. The green translucent surface represents a plane dipping 250/22, corresponding to the dip of the Salzberg thrust in outcrops (d) and (e). Compare the topographic intersection of this plane with the trace of the thrust mapped in (a). (c) Photograph of a monoclinical fold in the Dachstein Limestone located in the eastern Echernwand, above the entrance to the Hallstatt Erbstollen gallery. (d) View of the slope on the south of the Hallstatt Salzberg. (e) and (f) Views of the slope north of the Hallstatt Salzberg. (g) and (h) Views of the eastern slopes of the Hühnerkogel and Schneidkogel. Note that view (h) is from the north and the rock face observed is hidden in the view in (a). 1 = Trace of the Salzberg thrust; 2 = Salzberg thrust south of the Salzberg; 3 = possible location of a syncline in the footwall of the Salzberg thrust; 4 = estimated northeastern prolongation of the salt weld from Figure 6; 5 = possible location of an anticline; 6 = tight folding in the Dachstein Limestone; 7 = northern termination of the Salzberg thrust. Images (a), (d), (g) and (h) captured in GoogleMaps (captured 25 Jan. 2022; imagery from Geoimage Austria, CNES/Airbus, Maxar Technologies, Salzburg AG/Wenger Oehh). Image (b) includes overlay of the geological map of Schäffer et al. (1982). Image (c) courtesy of Prof. Nikolaus Froitzheim. Images (e) and (f) are orthophotographs of 3D outcrop models discussed in the text.

the Hallstättersee that have been observed, but not discussed, by previous authors.

The largest structure encountered in this area is called here the Salzberg thrust: a west-dipping thrust that crosses the upslope end of the Hallstatt Salzberg (label 1 in Fig. 11a). This thrust can be correlated along strike to other outcrops along the trace of what would correspond to a plane dipping 250/22 (red line in Fig. 11a; green surface in Fig. 11b). From south to north, the Salzberg thrust can be observed in outcrop as follows:

- 1) An east-vergent monoclinical fold is observed on the eastern end of the Echernwand (Fig. 11c) which most likely represents the southern termination of the thrust.
- 2) The thrust crops out on the southern slope of the Salzberg (Fig. 11d). The thrust here transports vertical dipping beds in its hanging wall that form a syncline (label 2) with NNW-SSE trend, perfectly along strike from the monocline in Figure 11c. The thrust is also overriding steeply dipping beds that contrast with the gentle dip further east. The link between both (label 3) cannot be understood from this outcrop view. Likewise, the prolongation of the weld structure from Figure 6 maps to a location similar to that marked by label 4, but this interpretation cannot be fully substantiated. The lack of homologous points makes it impossible to determine its displacement, but based on the offset of vertical beds, 50 to 100 m of minimum throw are possible.
- 3) The Salzberg thrust crops out also on the northern side of the Salzberg (Fig. 11e), separating panels of Dachstein Limestone with different dip (angularity also observed by Arnberger, 2006). On this outcrop, minor extensional faults, possibly syn-depositional, can also be seen.
- 4) Although not strictly linked with the Salzberg thrust, a tight, east-vergent overturned syncline is observed in the Dachstein Limestone on the easternmost end of the Salzberg north slope (Fig. 11f). However, the vergence indicated by this structure is in accord with the kinematic of the thrust and can be interpreted to be related to the same deformation process. It must

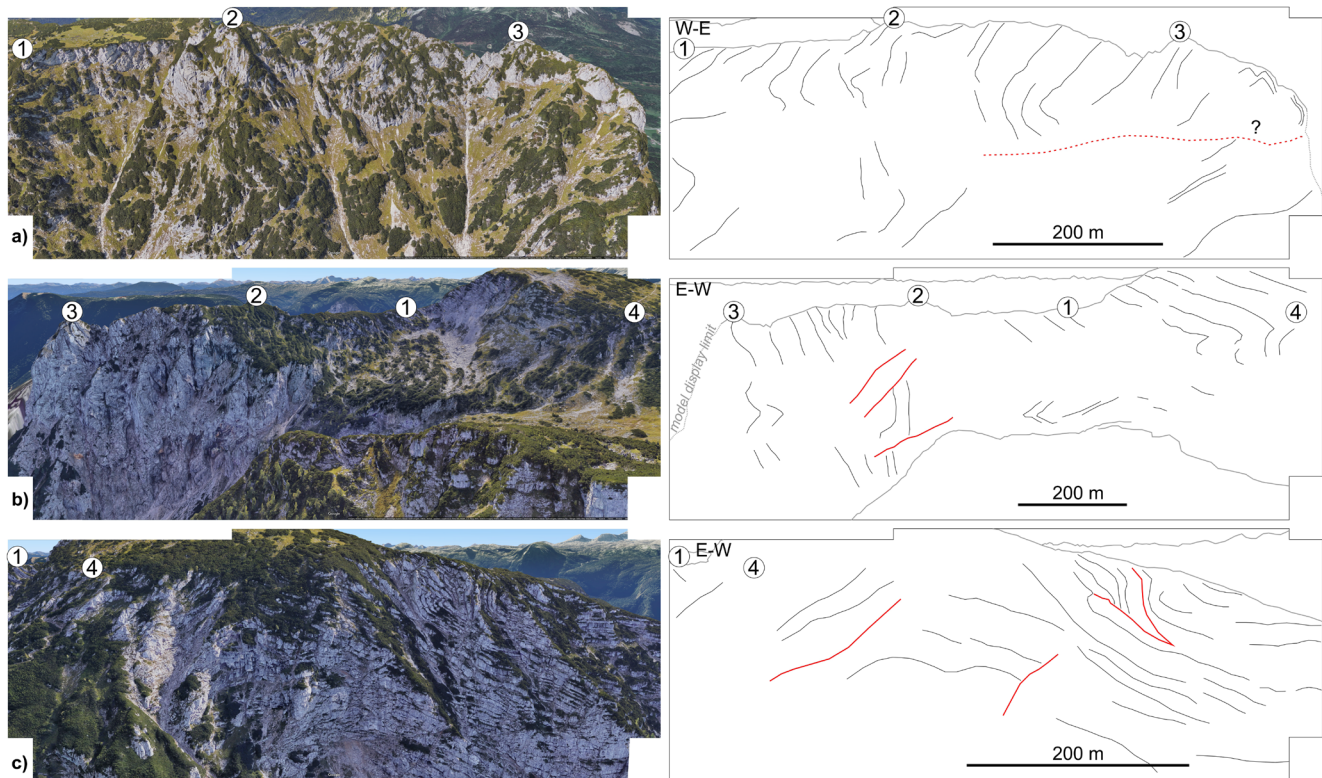


**Figure 12:** (a) View from the south of the ridge stretching east from the Hoher Sarstein (label 6 in Fig. 4) and its line drawing. (b) View from the north of the same ridge as in (a) and its line drawing. Note that the display in Google Maps fails to show the eastern end of the ridge in this view. (c) View from the north of the ridge stretching west from the Hoher Sarstein (label 7 in Fig. 4) and its line drawing. Equivalent points in the different images are shown as numbers 1 - 4 in the figure. All images captured from GoogleMaps (captured 25 Jan. 2022; imagery from Geoimage Austria, CNES/Airbus, Maxar Technologies, Salzburg AG/Wenger Oehn).

be noted however, that the fold is not seen in its entirety, and the outcrop does not reveal the anticline that would be expected updip from the syncline (label 5).

- 5) The thrust crops out once again a few hundred meters to the north (Fig. 11g) where tighter folding of the Dachstein Limestone is observed in the footwall of the thrust (label 6, Fig. 11g). These folds have a roughly N-S trend and can therefore be interpreted to be related to the same deformation process as the thrust. Although not pictured here, similar folds have been observed further down the slope (label 6 in Fig. 11a).
- 6) The thrust terminates northwards and at the location of Figure 11h is only seen as a tight, west-vergent detachment fold, whose position coincides with the projected position of the thrust (label 7).

The overall dimension of the thrust is limited (just over 1 km along strike) and the maximum throw is likely at most in the order of a 100 m. The thrust appears to also effectively use intra-formational detachments, as is inferred from the fact that both ends (Fig. 9c, h) present propagation anticlines that do not fold the entire thickness of the Dachstein Limestone.

Although not related to the thrust, a feature of this western slope of the Hallstättersee is the presence of

panels of Dachstein Limestone that dip steeply (over  $40^\circ$ ) towards the east. One such structural slope is observed under the Salzburg (at the position of label 8 in Fig. 11a), where topography follows the dip of the Dachstein Limestone (not visible in the image). Although this appears to be possibly an isolated feature, the geometry is reminiscent of the monocline in Obertraun and could indicate the presence of a N-S trending fault under the Hallstättersee, as mentioned in section 3.3. The eastward dipping monocline, however, indicates that the western block is lowered, leaving the Sarstein in a relatively elevated position in its footwall.

Another location of prominent shortening-related deformation is encountered on the other side of the Hallstättersee, around the Hoher Sarstein peak (Fig. 12). The ridge that stretches east of the Hoher Sarstein peak (Fig. 12a, label 6 in Fig. 4) presents verticalized Dachstein Limestone beds, cross-cut by a sub-horizontal (likely tilted) thrust. In addition to steep dips seen at the eastern end of the ridge, bedding is also significantly folded and its dip shallows progressively westwards. The northern flank of the ridge (Fig. 12b) presents a similar pattern, although thrusts are smaller than that observed on the south flank (Fig. 12a). On the ridge that leads east of the Hoher Sarstein (Fig. 12c, label 7 in Fig. 4), thrusting has even led to the development of a small-scale triangle

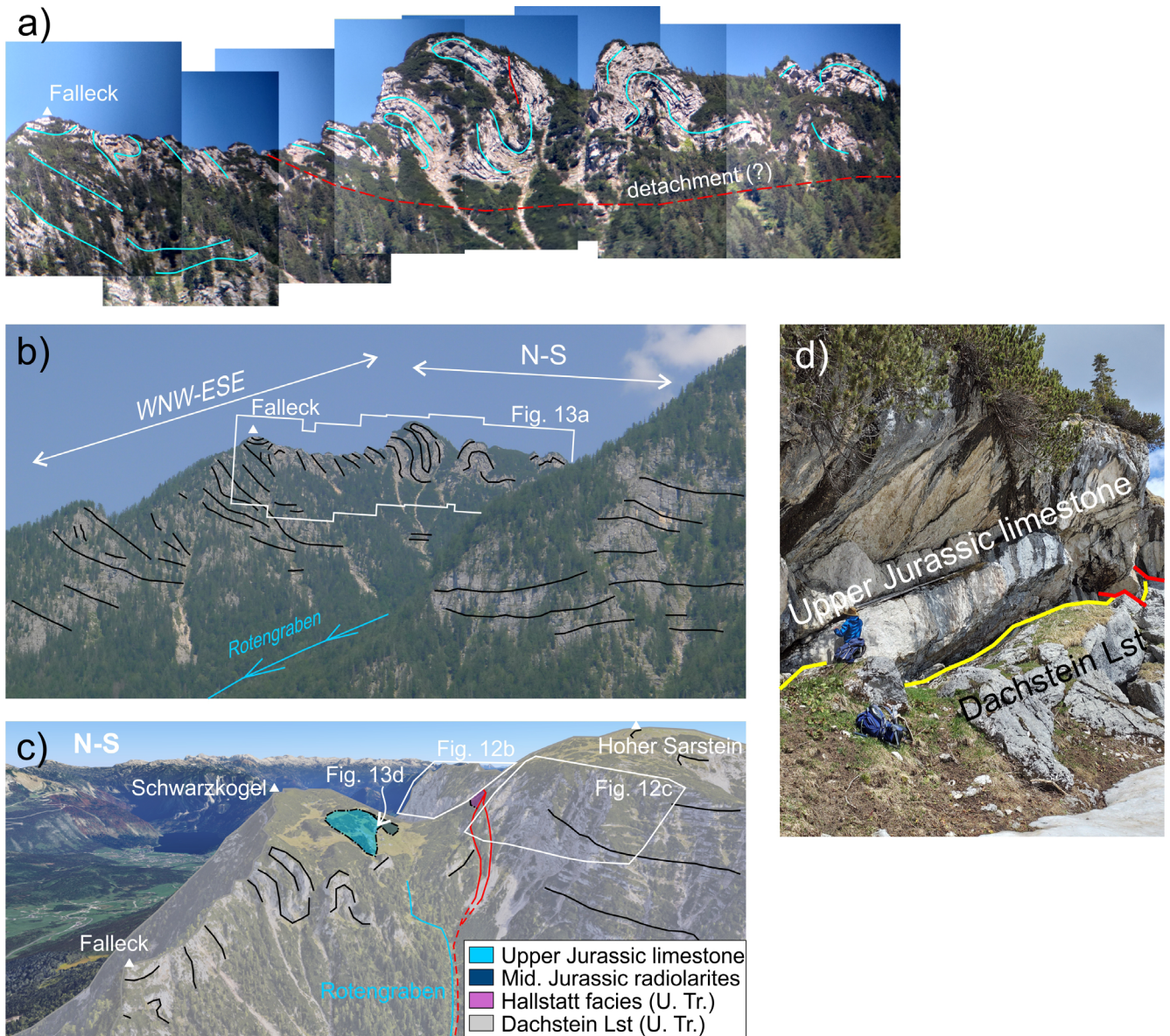


**Figure 13:** Panorama (b) and detail (a) of the Felleck ridge and folded Dachstein Limestone. The ridge trends roughly E-W over the Felleck and the outcrop turns to a N-S direction in its uppermost segment. See Figure 4 for location (label 8). The panorama and the detailed photos are taken with slightly differing perspectives that can be complemented with oblique perspective from Google Maps in (c). Above the Felleck folds, the Dachstein is overlain directly by Upper Jurassic reef-slope limestones (d) along a mostly conformable contact (yellow line) that is slightly faulted (red lines). The oblique image in (c) was captured 05 Jul. 2022 (imagery from Geoimage Austria, Maxar Technologies, Salzburg AG/Wenger Oehn, CNES/Airbus, Landsat/Copernicus, Data SIO, US Navy, NGA, GEBCO). The photo in (d) has the north to the left and William Munday stands against the outcrop for scale. Abbreviations: Lst = Limestone, Mid. = Middle, U.Tr. = Upper Triassic.

zone. Along this ridge, direction of thrusting is to the west, opposite that of the Salzberg thrust and associated structures. However, trend of the structures is observed to be roughly north-south, similar to that of the Salzberg thrust. And as with the Salzberg thrust, deformation does not involve the entire Dachstein Limestone in any of the structures observed, but rather thrusts and folds seem to use intra-formational detachments.

In contrast to the north-south trend of the structures on the Hoher Sarstein, the outcrop in the vicinity of the Felleck (label 8, Fig. 4) presents shortening structures with east-west fold axes (Fig. 13a-c). Also in contrast to

the structures on the Hoher Sarstein, the folds around the Felleck are mostly isoclinal and, at least for the highest part of the outcrop, appear to have a single bed-parallel detachment (Fig. 13a). The Sarsteinalm fault (label 7 in Fig. 9c; red line in Fig. 13c) separates the Felleck folds from the Hoher Sarstein structures (Fig. 13c). This fault, runs immediately north of the outcrop faces in Figure 12b, c, was active during the deposition of the Dachstein Limestone (as discussed previously), lowering the “Felleck block”. The coincidence in east-west trend, the fact that the folding of the Felleck is very unique in geometry and is restricted to the hanging wall of the Sarsteinalm normal

fault, and the Triassic age of this fault, make it reasonable to assume a genetic link between the fault and folding. In this sense, these folds could have been formed early after deposition or during early burial due to southward-directed slope instability caused by fault motion: down-dropping and rotation of the Rotengarben fault hanging wall would have caused beds in the Dachstein Limestone to slide into the fault and fold due to buttressing against the footwall. Outcrop accessibility has precluded the possibility of documenting the detachment for this sliding process, but it is interpreted in any case to be a lithologically controlled, bed-parallel detachment.

#### 4. Discussion of structures involving the Dachstein Limestone

In the previous section, four main types of structures have been discussed, based on their genesis:

- 1) Salt-driven structures (halokinetic hooks in Fig. 6);
- 2) Structures related to depositional instability (soft-sediment deformation; the folds of the Falleck ridge in Fig. 13).
- 3) Extensional faults that cross-cut the entire Triassic carbonate platform (faults of the Echerntal, of Obertraun and of the Sarsteinalm; Figs 8, 9 and 10); and
- 4) Shortening structures with vergence and kinematics to the east or to the west (N-S strike) (the Salzberg thrust in Fig. 11, and the Hoher Sarstein structures in Fig. 12).

Below we discuss their timing and the mechanism driving their formation.

##### 4.1 Salt-driven structures

The halokinetic hooks of the Echernwand provide unique insights into the development of halokinetic hooks. Whereas published examples tend to rely on map-based or partial outcrop observations (e.g., Giles and Rowan, 2012; Hearon et al., 2014; Poprawski et al., 2016; Vidal-Royo et al., 2021), the detail of the Echernwand outcrop makes it possible to observe details not previously described.

Composite halokinetic sequence development has been described in detail by Giles and Rowan (2012) and further refined by Poprawski et al. (2016) for carbonate-dominated systems. Giles and Rowan (2012) and Poprawski et al. (2016) noted that in shallow water carbonate-dominated systems, carbonates will aggrade readily above a rising diapir. The thick roof that results will lead to the development of tapered composite halokinetic sequences (CHSs) in which individual halokinetic sequences are wedge shaped and form relatively reduced angles with one another. Poprawski et al. (2016) proposed, however, that if sea level drop during LSTs (lowstand system tracts of Catuneanu et al., 2011) is sufficient, the roof of a diapir can be denuded and lead to the development of tabular CHSs, in which individual halokinetic sequences are tightly folded near the diapir

(forming hooks) and truncated at high angle by overlying sequences.

The stack of halokinetic sequences of the Echernwand conform a tabular CHS (Fernandez et al., 2021) and therefore correlate with a relative sea level lowstand in the model of Poprawski et al. (2016). Nonetheless, the geometry of the beds in the vicinity of the salt weld reveals subtleties in the evolution of individual halokinetic sequences. As discussed previously, individual halokinetic sequences of the Echernwand can be subdivided into two intervals (parasequences) exhibiting a varying relationship with respect to the diapir. The lower intervals in each sequence (1.1 and 2.1, Fig. 6b, c, e) exhibit geometries indicating that limestone beds partly onlapped and even locally overlay the rising diapir (Fig. 6c, e) in the form of a burial wedge (*sensu* Langford et al., 2022). In contrast, the upper intervals (1.2 and 2.2, Fig. 6b, d, f) exhibit offlapping geometries relative to the diapir as well as internal onlap and thinning (labels 2 and 5 in Fig. 6b; see also Fig. 3f in Fernandez et al., 2021). This progression within individual halokinetic sequences mimics, at a higher sequence order, the impact of relative sea level changes observed by Poprawski et al. (2016): higher relative sea level allows for carbonate to onlap and aggrade above the diapir (TST) in the base of each sequence (even if part of the diapir continues to be emergent) (Fig. 6c,e); dropping sea level leads to a forced regression (RST: regressive system tract in Catuneanu et al., 2011) at the top of each sequence (Fig. 6d,f). In this scheme, the boundary between two halokinetic sequences actually is the maximum regressive surface (MRS in Catuneanu et al., 2011) at the base of the TST. Folding in each halokinetic sequence occurs at the end of the RST, indicating that relative diapir rise (or minibasin subsidence) only becomes a major process during the RST, probably as a result of denudation of the diapir roof by erosion during sea level drop. This presents a system in which rising sea level can slow down diapir growth due to the aggradation of platform carbonates above the diapir. Dropping sea level, in contrast, enhances erosion of the diapir roof and therefore permits faster extrusion of salt. Uniformity in the facies of the lagoonal Dachstein Limestone in the Echernwand indicates that the cyclicity in sea level change and diapir activity was in equilibrium with the fine balance between subsidence of Dachstein Limestone basins and carbonate platform aggradation. This delicate balance, in spite of active salt tectonism, preserved the shallow water conditions recorded by the Lofer cyclothems for prolonged periods of time (in the order of 5 Ma for the Echernwand if one assumes 1500 m of Dachstein Limestone accumulated in roughly 15 Ma; Mandl, 2000).

##### 4.2 Soft-sediment deformation

In contrast to the examples of Giles and Rowan (2012) and Poprawski et al. (2016), no breccias have been observed in the halokinetic hooks of the Echernwand. At most, intraformational brecciation and fractures filled with lime

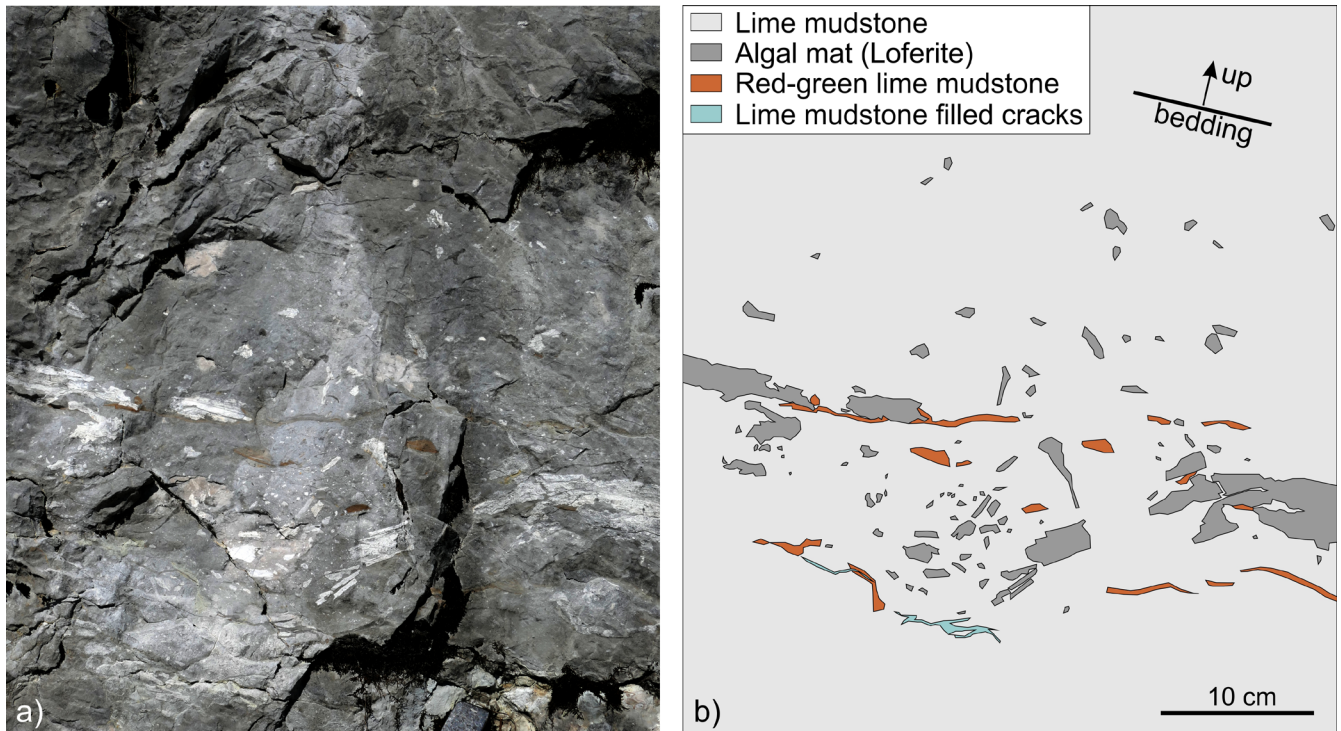


**Figure 14:** Photo (a) and interpretation (b) of a seismite in the Dachstein Limestone. A whitish bed of early-diagenetically dolomitized fenestral limestone (Loferite; Fischer, 1964) has been brittlely broken, with the angular fragments being displaced into a ductile (unlithified) lime-muddy matrix of the subtidal parts of the under- and overlying peritidal cycles. This structure shows that loferite levels of the Dachstein Limestone lithified more rapidly than subtidal lime muds of the peritidal cycles they are intercalated between. Fragments of red to greenish argillaceous limestone (member A of the Lofer cyclothems; Fischer, 1964; Tollmann, 1976) observed in Figure 14 can owe their scattered arrangement to, either, a primary irregular distribution (Fischer, 1964), or to deformation coeval with that of the loferite levels. See Figure 4 for location (label 9) (approx. 47°39.492'N, 13°47.048'E).

mudstone (e.g., Fernandez et al., 2021) show that some beds were partly lithified at the time of folding. However, no beds composed of angular pebbles to cobbles redeposited into subtidal lagoonal sediments have been encountered. This may be explained if the lagoonal carbonate sediments were not completely lithified at the time of folding and erosion, being re-worked into lime mud and/or silt- to sand-sized grains by wave action, instead of angular pebble- to cobble-sized components.

For the lagoonal Dachstein Limestone, a delayed lithification of the subtidal cycle portions relative to the inter- to supratidal levels is consistent with observations in equivalent Dachstein facies within the Tirolic thrust system (label 9 in Fig. 4). Figure 14 shows a seismite in a lagoonal Dachstein limestone succession; here, several intervals of early dolomitized loferites (or member B of the Lofer cyclothems; Fischer, 1964; see also Haas et al., 2015) became torn apart into angular fragments, indicating brittle fracturation occurred after lithification. The loferite fragments have been observed to float within lime-muddy matrices of the subtidal parts of the respective under- and overlying peritidal cycles. This downward and upward displacement of the loferite fragments can only be explained by liquidization (likely fluidization; Maltman and Bolton, 2003) of the surrounding lime mudstone during coseismic breakage. Cracks filled with lime mudstone towards the base of the image in Figure

14 indicate the likely base of unlithified material at the time of deformation. This pattern of fluidization and hydraulic shattering is very similar to that described in similar peritidal sequences by Etensohn et al. (2011).

This and multiple similar examples can be encountered towards the top of the Dachstein Limestone on the southern flank of Mount Loser. From the evidence at hand, we cannot assess how widespread this phenomenon was. However, soft-sediment deformation within the lagoonal Dachstein Limestone indicates that these sediments, at least locally, and at least in the youngest Dachstein Limestone, did not necessarily consolidate rapidly, as could otherwise be expected for tidal-flat carbonates (e.g. Shinn et al., 1969). The origin for this can be the presence of impermeable layers within the mud micrite (e.g., Etensohn et al., 2011) and/or the presence of cyclic loading due to repeat seismic events that enhance overpressure (Maltman and Bolton, 2003). Evidence for delayed consolidation has also been recently reported for the Wetterstein Limestone in the western NCA (Ortner, 2020), raising the possibility that this phenomenon may be relatively common. Furthermore, ductile coseismic deformation within cyclic peritidal successions is known also from the banktops of other carbonate platforms (e.g., Pratt, 2002; Spalluto et al., 2007).

Delayed consolidation of the lagoonal Dachstein Limestone can help account for geometries such as those

observed in the Falleck folds (Fig. 13a-c). As discussed above, the location of these folds in proximity to the Sarsteinalm fault, the orientation of fold axes parallel to the fault, the Triassic age of fault activity, make a genetic link between both likely. Furthermore, tightness in folding and the presence of undeformed beds above and below (Fig. 13c) makes this train of folds a strong candidate to have originated due to soft-sediment deformation (Elliott and Williams, 1988).

Although we have not encountered other unambiguous examples of soft-sediment deformation in the Dachstein Limestone within the Dachstein TS, various structures in the underlying Tirolic thrust sheet have been identified that show this is not an isolated phenomenon (Fig. 15). Examples of slump folding in the Dachstein Limestone, with folded beds overlain by regionally dipping, unfolded beds, have been encountered in the upper Dachstein Limestone in different locations, but consistently in the uppermost tens of meters of the Dachstein Limestone (as measured from the contact to overlying Jurassic units). For one, along the Naglsteig trail, east from the Rettenbach, a stratal package of lagoonal Dachstein beds roughly 10 m thick is folded and truncated by overlying beds (Fig. 15a). A second example is encountered east of the town of Bad Ischl, where multiple stacked folds within 70 m of the top of the Dachstein Limestone. In this case, Dachstein Limestone slumped into tight folds was posteriorly overlain by flat lying limestone beds that were in turn later folded into a broad anticline that was subsequently overlapped by younger beds (Fig. 15b). The truncated fold geometry and internal onlap relationships proves their syn-depositional nature of these structures (Elliott and Williams, 1988; Ortner and Kilian, 2016; Alsop et al., 2019).

Another example of soft-sediment deformation can be encountered at the contact between the Dachstein Limestone and the Upper Jurassic Oberalm Fm along the Grabenbach, southeast of the locality of Bad Ischl (Fig. 15c). This unconformity was already described by Mandl (2013) at this locality as removing a significant part of the uppermost Dachstein Limestone. The contact is characterized by a dip roughly parallel to that of the underlying Dachstein Limestone (labels 3 and 4, Fig. 15c) and the presence of meter-scale blocks of Dachstein Limestone within the Oberalm Fm immediately above. One of these blocks presents isoclinally folded beds (similar to the folds in Fig. 15b). Besides the fact that dissolution-precipitation processes alone cannot accommodate the strain in isoclinal fold hinges, the age gap between the Norian Dachstein Limestone and the Kimmeridgian to Tithonian Oberalm Fm (easily over 50 Ma) leads us to interpret that the folded Dachstein Limestone block is a remobilized fragment of a syn-depositional slump fold (similar to the re-sedimented soft-sediment folds of Alsop et al., 2019).

Finally, an outcrop along the Rettenbach, in the proximity of the previous outcrops (Fig. 13d) also presents structures within the Dachstein Limestone that

could be consistent with soft-sediment deformation. In this case, the side-by-side juxtaposition of contractional folding and pervasive extensional faulting likely implies that deformation occurred in a setting with limited confining stress, as in shallow burial. In this case, the lack of overlying beds makes it impossible to determine the age of folding. However, this fold occurs within the top 100 meters of the Dachstein Limestone and its roughly east-west trend implies north-south shortening that coexisted with extension, equivalent to the process that led to the development of the Falleck ridge folds.

### 4.3 Extensional faults

As is discussed in section 3.2, thickening of the Dachstein Limestone against the extensional faults of the Echerntal (Fig. 8, label 1 in Fig. 9c) indicates these faults were active during the Late Triassic. In the case of the Obertraun fault (label 3, Fig. 9c) there is no evidence for Triassic activity during deposition of the Dachstein Limestone (due to the constant thickness of this unit into the fault). In both cases, the top of the Dachstein Limestone is dropped in the order of hundreds of meters in the hanging wall of the faults (blocks to the north and northwest of the faults), an offset that is clearly observable in the present day topography (Figs. 9, 10). A major topographic step occurs across the Echerntal faults and its southwestern prolongation (Fig. 16a; labels 1 and 2 in Fig. 9c; red line in Fig. 9b) within the Dachstein Massif (see Fig. 9b and the elevations of peaks on either side of this fault in the map of Fig. 9c). In the vicinity of the Echerntal, the Dachstein Limestone is also intensely karstified (Fig. 9b, c), with karstic cavities filled in with Lower Jurassic age red mud limestone (age based on a sample with *Involutina liassica*, a Lower Jurassic index fossil; sampled at 47°32'11.15"N 13°36'13.55"E, Fig. 4). Karstification is so pervasive, that the Dachstein Limestone in this area has even been interpreted as a Jurassic breccia (Schäffer, 1982; Gawlick, 2007). However, the Dachstein Limestone dips consistently in large (hundreds of meters) undisturbed blocks (e.g., label 3, Fig. 8), and its beds are in physical and structural continuity with the Dachstein Limestone to the west (and not lying above it, as might be expected for a younger breccia). This implies that the pervasive presence of Jurassic red argillaceous limestone cement is better explained as the result of karstic infill than as resulting from the re-sedimentation of large (hectometric scale) blocks of the Dachstein Limestone in a Jurassic matrix (thus mapped as an area of karsting in Fig. 9c; compare with the map of Schäffer, 1982). The intense karstification of the Dachstein coincides with the area of the largest offset in the Echerntal faults. It is possible that karstification was enhanced by fracturing of the Dachstein due to fault activity, thus potentially indicating a Jurassic age of post-Triassic fault activity. Jurassic infill of Dachstein along discrete, NW-SE trending fissures up to 300 m deep has been documented in the Dachstein massif, in the footwall of the Echerntal faults (Mandl et al., 2012). However, it is not evident from the available



**Figure 15:** (a) Slumped beds of the Dachstein Limestone. Beyond the outcrop, beds dip strongly to the W (~270/50). Stratigraphic top is to the left in the photo. Beds at the top of the picture truncate the slumped beds (label 1). Folded beds are partly overturned and have a fold axis plunging roughly 45/050. See Figure 4 for location (label 10) (approx. 47°41.028'N, 13°45.150'E). (b) Slumped beds of the Dachstein Limestone in an area where the regional dip is sub-vertical (330/90) and with the top to the NW (to the left in the picture), as seen at the left end of the outcrop. In the outcrop beds are seen to be both gently folded into an originally up-right anticline that is onlapped from both sides (label 2). This fold involves in its core a set of tighter anticlines and synclines that trend NE-SW (roughly 00/060) and that are stratigraphically lower (to the right in the picture). See Figure 4 for location (label 11) (approx. 47°42.532'N, 13°40.118'E). (c) Contact between the Dachstein Limestone and the Upper Jurassic Oberalm Fm (label 3). Regional dip is towards the south (label 4). The Oberalm Fm is strongly slumped and contains olistoliths of Dachstein Limestone (labels 5). One of these is a fragment of isoclinally folded limestone (label 6). See Figure 4 for location (label 12) (47°41.904'N, 13°41.918'E). (d) Outcrop of deformed upper Dachstein Limestone including a detachment fold (label 7), a rotated panel (8) and abundant extensional structures (label 9). See Figure 4 for location (label 13) (47°41.223'N, 13°41.137'E). Coordinates are given in WGS84 datum and are approximate for (a) due to steepness of terrain.

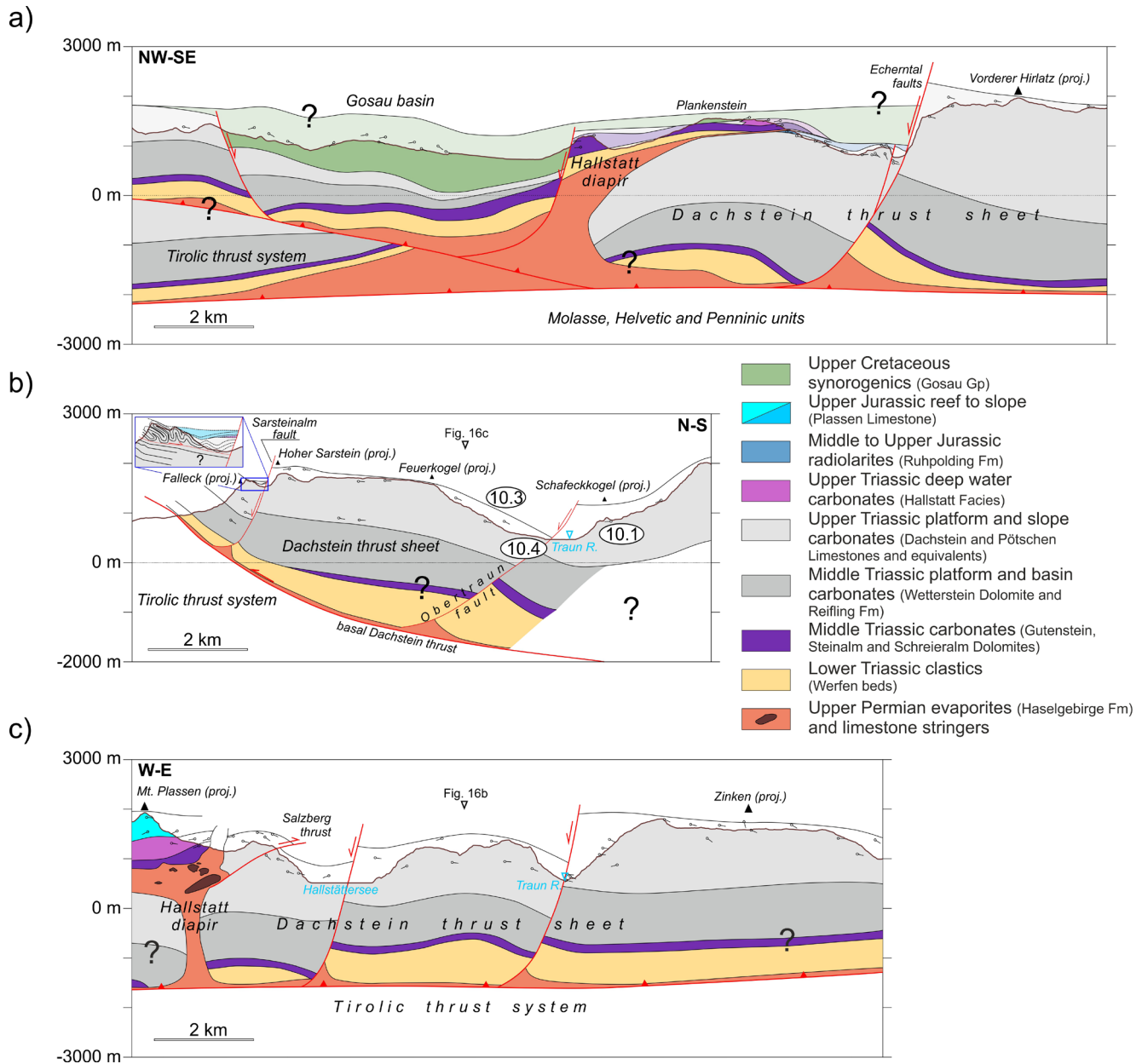


**Figure 16:** Cross-sections across the study area. **(a)** NW-SE trending section across the Echerntal faults and the Gosau basin. The extent of Gosau Gp sediments SE from the Gosau basin is uncertain, but extends certainly at least up to the Plankenstein. It is interpreted that both the Echerntal faults and the faults bounding the Gosau basin detach into the Permian evaporites at the base of the Dachstein thrust sheet. On the Plankenstein Lower Triassic carbonates and deep water Hallstatt facies that overlay the Hallstatt diapir have been thrust over the Dachstein Limestone during Late Jurassic times (Fernandez et al., 2022). **(b)** N-S trending section along the Sarstein, showing the Obertraun fault, the Sarsteinalm fault and the Falleck folds (in inset). The Sarsteinalm cross-cuts the entire Triassic stratigraphy (Fig. 4) and the Obertraun fault is interpreted to do the same by analogy. The entire system is transported northwards on the basal thrust of the Dachstein thrust sheet. Number labels indicate features labelled 1, 3 and 4 in Figure 10. **(c)** E-W trending section showing the relationship of the Salzberg thrust with the Hallstatt diapir and the faults along the Hallstättersee and the upper Traun valley. The internal structure of the Hallstatt diapir is derived from data provided by the Hallstatt mine operator Salinen AG (T. Leitner, pers. comm.). The Salzberg thrust is interpreted to cross-cut the Hallstatt diapir: although in this section it appears to root in the diapir, its relation to the diapir changes along strike, both to the north and the south. The interpretation at depth of all sections is uncertain and shaded to reflect this. See Figure 4 for location. The intersections between sections in (b) and (c) are shown on each section respectively.

data why karstification occurred more intensely (with the development of a broad karstic cavity network) in the lowered hanging wall block than in the (presumably) shallower footwall.

Beyond evidence for potential Jurassic activity on these faults, the Echerntal faults also caused a major offset in Jurassic sediments. Whereas on the Hirlatzwand

the Lower Jurassic of the footwall (now mostly eroded) is at around 2000 m elevation (Fig. 16a; label  $J_{FW}$  Fig. 9b), it lies below 1000 m elevation in the hanging wall of the Echerntal faults (Fig. 16a; label 4 in Fig. 8; label  $J_{HW}$  Fig. 9b). This offset points to Late Jurassic or post-Jurassic activity on the Echerntal faults. This could possibly relate to extension during the opening of the

Gosau basin for which faults are dated to have had Late Cretaceous activity (Wagreich and Decker, 2001) and have a similar southwest-northeast strike (Fig. 16a; label 8, Fig. 9c).

The southwest-northeast strike is also parallel to the salt weld of the Echernwand (Fig. 6, magenta line in Figure 9b-c). This coincidence, added to the fact that these extensional faults cross-cut the entire Dachstein Limestone unit (and based on their throw, almost certainly the entire underlying Triassic succession) and the proximity to the Hallstatt diapir (Fig. 9c), could mean that these are faults that detach within the evaporitic Permian Haselgebirge Fm (Fig. 16a).

By analogy with faulting in the Echerntal, and despite the lack of sediments to date activity it is possible that the Obertraun fault also post-dates the Lower Jurassic. The probable western prolongation of the Obertraun fault in the Echerntal valley (label 5 in Fig. 9c) lowers the Upper Jurassic of Mount Plassen (Fig. 9c) to elevations equivalent to that of the Upper Triassic in its footwall (Vorderer Hirlatz peak, Fig. 9c). This implies that activity on the Obertraun fault could be compatible with a phase of (Late?) Cretaceous collapse (as for the Gosau basin faults; Wagreich and Decker, 2001). The Upper Cretaceous infill that one would expect in the hanging wall half-graben would have likely been glacially eroded. Remnants are however preserved in the vicinity of the Hallstatt diapir: on the Solingerkogel (southeast of Mount Plassen) and on the Plankenstein (southwest of Mount Plassen, Fig. 16a). And similar to the Echerntal faults, this fault cross-cuts the entire Triassic platform sequence and likely detaches within the Late Permian Haselgebirge Fm evaporites (Fig. 16b). These observations mean that these extensional faults possibly relate to the collapse of underlying salt accumulations (and are also at least partly salt-driven features). Collapse could have occurred in successive stages and under varying stress regimes: in the Late Triassic (extension), in the Early (?) Jurassic (transtension?) and in the Late Cretaceous (transtension). Transtension in the Early Jurassic is compatible regionally with opening of the Penninic Ocean (Faupl and Wagreich, 1999) and in the Late Cretaceous with the development of the Gosau basin (Wagreich and Decker, 2001). However, Late Triassic extension has not been previously documented regionally but could relate locally to the collapse of the Hallstatt diapir.

An equivalent fault in terms of timing and nature is the Sarsteinalm fault running north of the Hoher Sarstein (Fig. 16b; label 7 in Fig. 9c), that lowered its northern fault block by a few hundred meters (Fig. 16b). This throw is enough to have led to the deposition of deep water Upper Triassic carbonates in the fault's hanging wall (as discussed in section 3.4 in relation to the Falleck ridge folds). As the Echerntal and Obertraun faults, the Hoher Sarstein fault cross-cuts the entire Triassic succession (Schäffer, 1982) (Fig. 16b). There is no strong evidence to suppose this fault had any post-Triassic activity, but it cannot be ruled out.

Finally, one last fault associated with extension in the area is one that runs roughly north-south along the Hallstättersee (Fig. 16c; label 6, Fig. 9c). This fault is inferred based on the eastward dips of the Dachstein Limestone west of the lake (Fig. 16c; label 8 in Fig. 11a) that would drop the Dachstein Limestone below its elevation on the eastern side of the lake. In contrast to the role as a termination for the fault east of the Sarstein (label 4, Fig. 9c), the fault in the Hallstättersee does not imply a termination of the Obertraun fault but simply compartmentalizes its hanging wall. The mismatch in the Dachstein Limestone between the eastern and western sides of the Hallstättersee could however also be solved with multiple faults with varying orientations, and possibly involving the northwest-southeast trending faults that define the northeastern limit of the Hallstatt diapir (Fig. 9c).

#### 4.4 Contractional structures

Tectonically driven contraction in the study area is dominated by two mutually perpendicular directions. At the regional scale, north-south shortening in the order of many kilometers is documented by thrusting of the Dachstein TS (Fig. 5; Fig. 16b). In contrast, small scale structures around the Hallstättersee are dominated by east-west directed shortening (Salzberg thrust, Fig. 16c, and Hoher Sarstein structures). This shortening direction was already documented by Habermüller (2005) and Schmid (2009). Amongst other structures, they identified shortening structures in the hangingwall of the Echerntal extensional faults that could be related to buttressing against its footwall during shortening. Schmid (2009) also identified the presence of the Salzberg thrust, but failed to recognize its lateral continuity. The east-west shortening described in this article and by Habermüller (2005) and Schmid (2009) is also consistent with the sealing of the salt weld of the Echernwand. Although precise direction of the relative motion between the blocks on both sides of this weld is not known, the presence of east-west directed shortening structures (label 7, Fig. 6b) and the fact that evaporites have been completely removed from the weld point to a significant component of weld-normal shortening (east-west to southeast-northwest directed).

Dating of these structures is ambiguous but is proposed by Schmid (2009) to be of Eo-Alpine age (Early Cretaceous) and pre-Gosau, partly based on the WNW-directed Eo-Alpine thrusting documented in the Austroalpine basement units (Ratschbacher, 1986; Ratschbacher and Neubauer, 1989; Schuster, 2003). No further evidence has been collected that would allow us to challenge or corroborate this assumption, but it is important to note that the E-W shortening direction contrasts with the north-directed transport of the Dachstein TS during Eo-Alpine deformation (Mandl et al., 2012) and the general NW-directed Eo-Alpine thrusting documented for the NCA (Linzer et al., 1995; Eisbacher and Brandner, 1996; Ortner and Kilian, 2022).

## 5. Implications

The observations of deformation affecting the Dachstein Limestone have implications on various aspects discussed below.

### 5.1 Late Triassic tectonic instability & salt tectonism

Deformation of the Dachstein Limestone during deposition or early burial indicates the presence of at least two important processes during Late Triassic times: salt tectonism and extensional fault activity. On the one hand, the development of the halokinetic sequences is unambiguous evidence for salt tectonism (at least in the Hallstatt diapir), as already described by Fernandez et al. (2021). This implies that the Dachstein Limestone was, at least partly, deposited within basins that subsided into underlying Permian salt (Haselgebirge Fm) that extruded to the surface along diapirs or other salt structures. These basins include older Triassic units (Wetterstein and Gutenstein carbonates), that do not crop out widely in the study area. However, based on our current understanding that salt structures grow mostly through passive diapirism (rather than through piercement; Rowan and Giles, 2021, and references therein) it is reasonable to expect that older Triassic units were also deposited with coeval salt tectonism. This has already been postulated by Strauss et al. (2021) and could explain the onlap of Dachstein Limestone onto the Wetterstein Dolomite and the thinning observed in the southern limb of the Weissenbach anticline (Fig. 5b, d).

On the other hand, the presence of extensional faults of Late Triassic age (Echerntal faults, Sarsteinalm fault) is indicative of tectonically-driven subsidence during this time. Furthermore, gravity-driven soft-sediment deformation (slumping) in the Dachstein Limestone, even in areas with no documented extensional faulting in the Tirolic units, requires a mechanism for the tilting of the sediment pile and generation of gradients that could trigger down-slope sliding. Given their temporal coexistence, both extensional faulting and tilting possibly relate to one same process driving localized extension and/or subsidence. Salt tectonics could provide an adequate mechanism for the generation of localized subsidence, through the collapse of salt structures or the lateral mobility of salt, but other mechanisms cannot be ruled out.

Whatever its origin, Late Triassic extensional faulting could potentially account for the presence of Hallstatt facies above the Dachstein Limestone in the Hoher Sarstein through the generation of deep water settings (hundreds of meters) within the domain of the Dachstein platforms. This possibility warrants further exploration and escapes the scope of this paper.

### 5.2 Post-Triassic collapse and strike-slip

Beyond extension and subsidence during the Late Triassic, the extensional faults cross-cutting the Dachstein Limestone (and older units) in the Dachstein TS are testimony to a phase of post-Triassic collapse.

Timing of this event is, in spite of its magnitude, not fully constrained. As discussed above, this collapse is regionally similar in magnitude to that documented for the Gosau basin by Wagneich and Decker (2001). This raises the question of the relevance of strike-slip (transtension) in the structure of the Dachstein TS, as Wagneich and Decker (2001) proposed the development of the Gosau basin as a pull apart basin between the left-lateral NW-SE striking Gosausee fault to the southwest, and a parallel left-lateral fault running along the northern edge of the Hallstatt diapir (called the Rötengraben fault by Mandl et al., 2012) to the northeast. The Rötengraben fault is also parallel to the fault documented along the Hallstatt Salzberg by Arnberger (2006). However, both of these faults, despite their strike-slip component, appear to be of limited regional relevance. Offset on the Rötengraben fault for instance, is interpreted to die out rapidly towards the east (as constrained by borehole data from the Hallstatt mine discussed by Suzuki and Gawlick, 2009, and Mandl et al., 2012). Likewise, the strike-slip fault of the Salzberg is right-lateral (Arnberger, 2006) opposite to slip on the Rötengraben fault, and does not cause any significant offset to the Salzberg thrust described above.

The limited magnitude of strike-slip observed along the northern edge of the Hallstatt diapir, the westward increasing throw on the Rötengraben fault (Wagneich and Decker, 2001; Mandl et al., 2012), and the proximity of the Gosau basin with the Hallstatt diapir might indicate that mechanisms other than only transtension could be at play in the development of the Gosau basin. For instance, extensionally (or transtensionally) aided collapse of salt bodies (e.g., Vendeville and Jackson, 1992; Jackson and Hudec, 2017) underlying the Triassic strata (as discussed for Late Triassic faulting) could provide a reasonable mechanism for the observed throw variations, limited strike-slip and magnitude of subsidence. Confirming the role of salt in the development of the Gosau basins and the broader post-Triassic subsidence requires further work and is, once again, not in the scope of this article.

### 5.3 Origin of E-W shortening

As discussed above, shortening in an E-W direction in the Dachstein TS is not necessarily consistent with the generally accepted NW direction of Eo-Alpine thrusting nor the N to NE direction of later thrusting (Linzer et al., 1995; Eisbacher and Brandner, 1996; Ortner and Kilian, 2022). The structures accommodating E-W shortening in the Dachstein Limestone are not pervasive and so far have been only documented in the Dachstein TS. However, similar N-S trending shortening structures are also present in other parts of the NCA. A prime example is the NNW-SSE trending Rossfeld syncline and the NW-SE striking and vertical dipping Barmstein beds (Upper Jurassic megabreccias) immediately west of the Salzach River valley and involving up to Lower Cretaceous sediments (Plöchinger 1987; Plöchinger et al., 1990), some 30 km west of the study area. Immediately across the Salzach River valley, Upper Jurassic and Lower

Cretaceous rocks are also folded into a NNW-SSE trending gentle syncline (Sankt Koloman syncline; Plöching et al., 1990). Verticalized beds of the Upper Cretaceous Gosau Group with a N-S strike can also be seen some 40 km to the east of the study area, immediately west of the Spital am Pyhrn locality (Moser and Pavlik, 2014). The examples of the Salzach valley are compatible with an Eo-Alpine deformation phase, but that from the Pyhrn area is younger. Irrespective of their timing, these N-S trending structures occur in the vicinity of known salt accumulations: the structures in this article are near the Hallstatt diapir, those in the Salzach valley are immediately adjacent to the Hallein-Bad Dürrnberg diapir, and those in Pyhrn are on the eastern flank of the Wurzeralm diapir. It is therefore one possibility that shortening involving salt bodies could help explain the presence of shortening structures developing even at right angles to the regional transport directions (e.g., Duffy et al., 2018).

#### 5.4 Deformation within the Hallstatt diapir

A question that naturally arises in view of all the structures discussed in the text, and their proximity to the Hallstatt diapir, is whether the internal structure of the diapir (e.g., as described by Habermüller, 2005; Schorn and Neubauer, 2014) reflects the structures observed in the Dachstein Limestone. Although the concept is appealing, strain recorded within the diapir does not necessarily correspond to strain experienced outside it. On the one hand, rapid re-crystallization of evaporites, even under reduced strain implies that structures can be readily overprinted. Indeed, Schorn and Neubauer (2014) indicate that structure within the Hallstatt diapir is strongly dominated by the latest phase of N-S directed shortening. On the other hand, flow within diapirs is highly complex and responds not only to horizontal tectonics (e.g., Strozyk et al., 2012; Jackson et al., 2015; Dooley et al., 2015). Therefore, a full understanding of the link between extra-diapir and intra-diapir deformation would require a more complete understanding of the 3D deformation pattern in the diapir (not solely in map view), mechanical layering within the evaporite body, and the full 3D geometry of the salt diapir walls and stringers.

#### 5.5 Present-day topography

The topography of the central NCA is dominated by the outcrop of the Dachstein Limestone and the time equivalent Hauptdolomit. These units form a really extensive slab of relatively flat-lying or gently dipping rock (e.g., Fig. 3) in spite of the thrust imbrication characteristic of the NCA. A possible reason for this surprisingly flat disposition is the presence of an efficient and significantly thick detachment (the Haselgebirge Fm) at the base of the NCA thrust sheets that favored coherent gliding of the entire Triassic to Jurassic carbonate sedimentary pile, with only limited internal deformation or major imbrication. Irrespective of the reason, the Dachstein Limestone and Hauptdolomit have proven to be units strongly resistant to erosion, in part aided by

the fact that precipitation and melt water easily infiltrate the karst systems of the carbonate massifs, leaving the top surface relatively undisturbed (Frisch et al., 2001). These units were even likely at one point buried under Cretaceous age sediments (as proven by the presence of Lower Cretaceous units atop isolated peaks such as the Solingerkogel or Mount Plassen (Schäffer, 1982; Gawlick and Schlagintweit, 2006) that rise hundreds of meters above the surrounding Dachstein Limestone. However, Cretaceous sediments, of weaker clastic lithologies, are generally absent and can be assumed to have been mostly eroded, with the hard substrate of the Dachstein Limestone dominantly defining topography in the area

As a result, the top surface of the massifs has evolved through the concentration of surface water flow along structurally controlled features. An excellent example for this is the U-shaped geometry of the Traun River valley east of the Hallstatt diapir (Fig. 9c), where it flows south along the tear fault east of the Sarstein, then turns west along the Obertraun fault, and then turns north again along the Hallstättersee where another tear fault has been inferred. Likewise, the Echerntal Valley coincides with a probable E-W trending fault just east of the village of Hallstatt (Fig. 9) and the major topographic step in the northwestern Dachstein massif (Fig. 9a, b) is controlled by the Echerntal faults. Although the relationship between topography and structure is not necessarily unambiguous, the correlation encountered in the study area indicates that it can be a useful criterion in exploring for major structures in other sectors of the central NCA.

#### 6. Conclusions

The Dachstein Limestone of the Dachstein thrust sheet presents multiple examples of small- to large-scale deformation. These structures are testimony to:

- 1) Syn-depositional folding of the Dachstein Limestone related to growth of the Hallstatt diapir;
- 2) Syn-depositional extensional faulting leading to the development of growth wedges in the Dachstein Limestone;
- 3) Syn-depositional, soft-sediment deformation (slumping) of the uppermost Dachstein Limestone related to extensional deformation;
- 4) Jurassic to Late Cretaceous extensional subsidence of large panels of the Triassic platform succession (Dachstein Limestone and underlying units) along kilometer-scale extensional faults, in a multi-phase process with varying tectonic drivers.
- 5) Early Cretaceous age shortening in an east-west direction, perpendicular to the possibly coeval, general northward transport direction of the Dachstein thrust sheet.

This article provides, to our knowledge, the first description of soft-sediment deformation within the Dachstein Limestone, as well as a timing and origin for the extensional structures along the northern Dachstein Massif.

The origin of many of the structures presented remains to be confirmed in greater detail. However, the complexity in the deformation pattern and history is compatible with the prolonged role of the basal Permian salt unit in controlling structural development of the area, from Triassic diapiric growth and basin subsidence, through Jurassic and Cretaceous fault-controlled subsidence and oblique contraction, to present-day topography of the study area. Finally, the analysis of halokinetic sequences of the Hallstatt diapir have made it possible to describe in unprecedented detail the development of halokinetic hooks in tabular composite halokinetic sequences in carbonate dominated systems.

### Acknowledgments

Research by O. Fernandez is supported by FFG and Salinen AG through the FFG-Bridge Project ETAPAS (FO999888049), FWF Project POLARIS (I 5399-N), and by NiMBUC Geoscience. The authors wish to thank Nikolaus Froitzheim for kindly allowing the publication of his photograph of the Echernwand monoclinial fold and Thomas Leitner from Salinen AG for providing the 3D model of the Hallstatt salt mine. Petex are thanked for academic license access to IPM-Move, which was used to obtain dip measurements from 3D outcrops and to prepare some images and cross-sections. The reviews by Hugo Ortner, Christoph Leitner and Jonas Kley helped to greatly improve an early version of the manuscript.

### References

- Alsop, G.I., Weinberger, R., Marco, S., Levi, T., 2019. Identifying soft-sediment deformation in rocks. *Journal of Structural Geology*, 125, 248–255. <https://doi.org/10.1016/j.jsg.2017.09.001>
- Arnberger, K., 2006. Detachment folding above the Permian Haselgebirge: Palinspastic reconstruction of alpine west-directed thrusting (Plassen, Hallstatt, Upper Austria). MSc Thesis, University of Vienna, Austria, 100 pp.
- Cataneanu, O., Galloway, W.E., Kendall, C.G.St.C., Miall, A.D., Posamentier, H.W., Strasse, A., Tucker, M.E., 2011. Sequence stratigraphy: Methodology and nomenclature. *Newsletters on Stratigraphy*, 44, 173–245. <https://doi.org/10.1127/0078-0421/2011/0011>
- Dooley, T.P., Jackson, M.P.A., Jackson, C.A.-L., Hudec, M.R., Rodriguez, C.R., 2015. Enigmatic structures within salt walls of the Santos Basin-Part 2: Mechanical explanation from physical modelling. *Journal of Structural Geology*, 75, 163–187. <https://doi.org/10.1016/j.jsg.2015.01.009>
- Duffy, O.B., Dooley, T.P., Hudec, M.R., Jackson, M.P.A., Fernandez, N., Jackson, C.A.-L., Soto, J.I., 2018. Structural evolution of salt-influenced fold-and-thrust belts: A synthesis and new insights from basins containing isolated salt diapirs. *Journal of Structural Geology*, 114, 206–221. <https://doi.org/10.1016/j.jsg.2018.06.024>
- Eisbacher, G.H., Brandner, R., 1996. Superposed fold-thrust structures and high-angle faults, Northwestern Calcareous Alps, Austria. *Eclogae geologicae Helveticae*, 89, 553–571. <https://doi.org/10.5169/seals-167913>
- Elliott, C.G., Williams, P.F., 1988. Sediment slump structures: a review of diagnostic criteria and application to an example from Newfoundland. *Journal of Structural Geology*, 10, 171–182. [https://doi.org/10.1016/0191-8141\(88\)90114-9](https://doi.org/10.1016/0191-8141(88)90114-9)
- Ettensohn, F.R., Zhang, C., Gao, L., Lierman, R.T., 2011. Soft-sediment deformation in epicontinental carbonates as evidence of paleoseismicity with evidence for a possible new seismogenic indicator: Accordion folds. *Sedimentary Geology*, 235, 222–233. <https://doi.org/10.1016/j.sedgeo.2010.09.022>
- Faupl, P., Wagneich, M., 1999. Late Jurassic to Eocene palaeogeography and geodynamic evolution of the Eastern Alps. *Mitteilungen der Österreichischen Geologischen Gesellschaft*, 92, 79–94.
- Fernandez, O., Habermüller, M., Grasemann, B., 2021. Hooked on salt: Rethinking Alpine tectonics in Hallstatt (Eastern Alps, Austria). *Geology*, 49, 325–329. <https://doi.org/10.1130/G47981.1>
- Fernandez, O., Grasemann, B., Ortner, H., Leitner, T., 2022. The Lower Juvavic of the Eastern Alps: Tectonic mélange or salt-controlled carbonate deposition? TSK 19 - 19th Symposium Tectonics - Structural Geology - Crystalline Geology; Halle (Saale), Germany, March 9–11.
- Fischer, A. G., 1964. The Lofer Cyclothems of the Alpine Triassic. In: Merriam, D.F. (ed.), *Symposium on Cyclic Sedimentation*. Kansas Geological Survey Bulletin. Kansas Geological Survey, 169, pp. 107–149.
- Frisch, W., Kuhlemann, J., Dunkl, I., Székely, B., 2001. The Dachstein paleosurface and the Augenstein Formation in the Northern Calcareous Alps – a mosaic stone in the geomorphological evolution of the Eastern Alps. *International Journal of Earth Sciences*, 90, 500–518. <https://doi.org/10.1007/s005310000189>
- Froitzheim, N., Plašienka, D., Schuster, R., 2008. Alpine tectonics of the Alps and Western Carpathians. In: McCann, T. (ed.), *The Geology of Central Europe Volume 2: Mesozoic and Cenozoic*. Geological Society, London, 1141–1232. <https://doi.org/10.1144/CEV2P.6>
- Gawlick, H.-J., 2007. Revision der Grünanger-Schichten (Schäffer, 1982) im Salzkammergut. *Arbeitstagung der Geologischen Bundesanstalt*, 2007, 159–164.
- Gawlick, H.-J., Schlagintweit, F., 2006. Berriasian drowning of the Plassen carbonate platform at the type-locality and its bearing on the early Eoalpine orogenic dynamics in the Northern Calcareous Alps (Austria). *International Journal of Earth Science*, 95, 451–462. <https://doi.org/10.1007/s00531-005-0048-4>
- Giles, K.A., Rowan, M.G., 2012. Concepts in halokinetic-sequence deformation and stratigraphy. In: Alsop, G.I., Archer, S.G., Hartley, A.J., Grant, N.T., Hodgkinson, R. (eds.), *Salt Tectonics, Sediments and Prospectivity*. Geological Society, London, Special Publications. Geological Society, London, 363, pp. 7–31. <https://doi.org/10.1144/SP363.2>
- Haas, J., Lukoczki, G., Budai, T., Demény, A., 2015. Genesis of Upper Triassic peritidal dolomites in the Transdanubian Range, Hungary. *Facies*, 61, 8. <https://doi.org/10.1007/s10347-015-0435-7>

- Habermüller, M., 2005. West-directed thrusting in the Dachstein Nappe: Quantification of eo-Alpine deformation around the Echerntal valley (Hallstatt, Austria). MSc Thesis, University of Vienna, 87 pp.
- Hearon IV, T.E., Rowan, M.G., Lawton, T.F., Hannah, P.T., Giles, K.A., 2014. Geology and tectonics of Neoproterozoic salt diapirs and salt sheets in the eastern Willouran Ranges, South Australia. *Basin Research*, 27, 183–207. <https://doi.org/10.1111/bre.12067>
- Jackson, C.A.-L., Jackson, M.P.A., Hudec, M.R., Rodriguez, C.R., 2015. Enigmatic structures within salt walls of the Santos Basin Part 1: Geometry and kinematics from 3D seismic reflection and well data. *Journal of Structural Geology*, 75, 135–162. <https://doi.org/10.1016/j.jsg.2015.01.010>
- Jackson, M.P.A., Hudec, M.R., 2017. *Salt Tectonics: Principle and Practice*. Cambridge University Press, Cambridge, 494 pp. <https://doi.org/10.1017/9781139003988>
- Krenmayr, H.G., Schnabel, H.-J., 2006. *Geologische Karte von Oberösterreich*, Geologische Bundesanstalt, scale 1:200,000.
- Langford, R.P., Giles, K.A., Rowan, M.G., McFarland, J., Heness, L., Lankford-Bravo, D., Thompson Jobe, J., Soltero, A., Bailey, C., 2022. Burial wedges—Evidence for prolonged progressive burial of the Paradox Basin salt walls—With a detailed example from Gypsum Valley, Colorado. *Basin Research*, 34, 1244–1267. <https://doi.org/10.1111/bre.12658>
- Leitner, C., Spötl, C., 2017. The Eastern Alps: Multistage development of extremely deformed evaporites. In: Soto, J.I., Flinch, J.F., Tari, G. (eds.), *Permo-Triassic Salt Provinces of Europe, North Africa and the Atlantic Margins*. Elsevier, Amsterdam, 467–482. <https://doi.org/10.1016/B978-0-12-809417-4.00022-7>
- Linzer, H.-G., Ratschbacher, L., Frisch, W., 1995. Transpressional collision structures in the upper crust: the fold-thrust belt of the Northern Calcareous Alps. *Tectonophysics*, 242, 41–61. [https://doi.org/10.1016/0040-1951\(94\)00152-Y](https://doi.org/10.1016/0040-1951(94)00152-Y)
- Maltman, A.J., Bolton, A., 2003. How sediments become mobilized. In: van Rensbergen, P., Hillis, R.R., Maltman, A.J., Morley, C.K. (eds.), *Subsurface Sediment Mobilization*. Geological Society, London, Special Publications. Geological Society, London, 216, 9–20. <https://doi.org/10.1144/GSL.SP.2003.216.01.02>
- Mandl, G.W., 2000. The Alpine sector of the Tethyan shelf – Examples of Triassic to Jurassic sedimentation and deformation from the North Calcareous Alps. *Mitteilungen der Österreichischen Geologischen Gesellschaft*, 92, 61–77.
- Mandl, G.W., 2003. Hallstätter Kalke auf dem Sarstein? (Salzkammergut, Oberösterreich). *Jahrbuch der geologischen Bundesanstalt*, 143, 213–220.
- Mandl, G.W., van Husen, D., Lobitzer, H., 2012. Erläuterung zu Blatt 96 Bad Ischl. Geologische Bundesanstalt, Vienna, Austria, 215 pp.
- Mandl, G.W., 2013. Zur Geologie des Raumes Hütteneckalm–Sandlingalm–Blaa-Alm (Salzkammergut, Österreich) mit kritischen Anmerkungen zur Sandlingalm-Formation. *Jahrbuch der Geologischen Bundesanstalt*, 153, 33–74.
- Medwenitsch, W., Schauburger, O., 1951. Tafel X: Hallstätter Salzberg. In: Heißel, W., and Exner, C., eds., *Geologischer Führer zu den Exkursionen: aus Anlaß der Wiederaufbau- und Hundertjahrfeier der Geologischen Bundesanstalt am 12. Juni 1951: Als Festgabe den an den Exkursionen teilnehmenden Geologen von den Mitarbeitern der Geologischen Bundesanstalt gewidmet*. Verlag der Geologischen Bundesanstalt, Vienna, Tafel X. (available at: [https://opac.geologie.ac.at/ais312/dokumente/VS0001\\_001\\_A.pdf](https://opac.geologie.ac.at/ais312/dokumente/VS0001_001_A.pdf))
- Moser, M., Pavlik, W., 2014. Blatt 98 Liezen 1:50.000. In: *Geologische Karte der Republik Österreich 1:50.000, Nr. 98*, Verlag der Geologischen Bundesanstalt, Vienna.
- Ortner, H., 2007. Styles of soft-sediment deformation on top of a growing fold system in the Gosau Group at Muttekopf, Northern Calcareous Alps, Austria: Slumping versus tectonic deformation. *Sedimentary Geology*, 196, 99–118. <http://doi.org/10.1016/j.sedgeo.2006.05.028>
- Ortner, H., Kilian, S., 2016. Sediment creep on slopes in pelagic limestones: Upper Jurassic of Northern Calcareous Alps, Austria. *Sedimentary Geology*, 344, 350–363. <https://doi.org/10.1016/j.sedgeo.2016.03.013>
- Ortner, H., 2020. Bericht 2018 über geologische Aufnahmen im Karwendelgebirge auf den Blättern UTM NL 32-03-17 Hinterriß und UTM NL 32-03-23 Innsbruck. *Jahresbuch der Geologischen Bundesanstalt*, 132, 392–396.
- Ortner, H., Kilian, S., 2022. Thrust tectonics in the Wetterstein and Mieming mountains, and a new tectonic subdivision of the Northern Calcareous Alps of Western Austria and Southern Germany. *International Journal of Earth Sciences*, 111, 543–571. <https://doi.org/10.1007/s00531-021-02128-3>
- Plöchinger, B. (ed.), 1982. Blatt 95 Sankt Wolfgang 1:50.000. In: *Geologische Karte der Republik Österreich 1:50.000, Nr. 95*, Verlag der Geologischen Bundesanstalt, Vienna.
- Plöchinger, B. (ed.), 1987. Blatt 94 Hallein 1:50.000. In: *Geologische Karte der Republik Österreich 1:50.000, Nr. 94*, Verlag der Geologischen Bundesanstalt, Vienna.
- Plöchinger, B., Brandecker, H., Leditzky, H.P., Maurin, V., Tichy, G., van Husen, D., 1990. Erläuterungen zu Blatt 94 Hallein. *Geologische Bundesanstalt, Vienna, Austria*, 76 pp.
- Poprawski, Y., Basile, C., Jaillard, E., Gaudin, M., Lopez, M., 2016. Halokinetic sequences in carbonate systems: An example from the middle Albian bakio breccias formation (Basque Country, Spain). *Sedimentary Geology*, 334, 34–52. <https://doi.org/10.1016/j.sedgeo.2016.01.013>
- Pratt, B.R., 2002. Tepees in peritidal carbonates: origin via earthquake-induced deformation, with example from the Middle Cambrian of western Canada. *Sedimentary Geology*, 153, 57–64. [https://doi.org/10.1016/S0037-0738\(02\)00318-4](https://doi.org/10.1016/S0037-0738(02)00318-4)

- Ratschbacher, L., 1986. Kinematics of Austro-Alpine cover nappes: Changing translation path due to transpression. *Tectonophysics*, 125, 335–356. [https://doi.org/10.1016/0040-1951\(86\)90170-8](https://doi.org/10.1016/0040-1951(86)90170-8)
- Ratschbacher, L., Neubauer, F., 1989. West-directed decollement of Austro-Alpine cover nappes in the eastern Alps: geometrical and rheological considerations. In: Coward, M.P., Dietrich, D., Parker, R.G. (eds.), *Alpine Tectonics*. Geological Society, London, Special Publications. Geological Society, London, 45, 243–262. <https://doi.org/10.1144/GSL.SP.1989.045.01.14>
- Rowan, M.G., Giles, K.A., 2021. Passive versus active salt diapirism. *AAPG Bulletin*, 105, 53–63. <http://doi.org/10.1306/05212020001>
- Schäffer, G. (ed.), 1982. Blatt 96 Bad Ischl 1:50.000. In: *Geologische Karte der Republik Österreich 1:50.000, Nr. 96*, Verlag der Geologischen Bundesanstalt, Vienna.
- Schlagintweit, F., Gawlick, H.-J., 2006. *Sarstenia babai* n. gen., n. sp., a new problematic sponge (inozoa?) from the Late Jurassic of the Northern Calcareous Alps, Austria. *Rivista Italiana di Paleontologia e Stratigrafia*, 112, 251–260.
- Schmid, S.M., Bernoulli, D., Fügenschuh, B., Matenco, L., Schefer, S., Schuster, R., Tischler, M., Ustaszewski, K., 2008. The Alpine-Carpathian-Dinaridic orogenic system: correlation and evolution of tectonic units. *Swiss Journal of Geoscience*, 101, 139–183. <https://doi.org/10.1007/s00015-008-1247-3>
- Schmid, N., 2009. Detachment Folding and Salt Tectonics in the Permian Haselgebirge (Hallstatt, Northern Calcareous Alps). MSc Thesis, University of Vienna, Vienna, Austria, 102 pp. <https://theses.univie.ac.at/detail/6387>
- Schorn, A., Neubauer, F., 2014. The structure of the Hallstatt evaporite body (Northern Calcareous Alps, Austria): A compressive diapir superposed by strike-slip shear? *Tectonophysics* 60, 70–84. <https://doi.org/10.1016/j.jsg.2013.12.008>
- Schuster, R., 2003. Das eo-Alpine Ereignis in den Ostalpen: Plattentektonische Situation und interne Struktur des Ostalpinen Kristallins. Arbeitstagung der Geologischen Bundesanstalt, 2003, 141–159.
- Schuster, R., Egger, H., Krenmayr, H.-G., Linner, M., Mandl, G.W., Matura, A., Nowotny, A., Pascher, G., Pestal, G., Pistotnik, J., Rockenschaub, M., Schnabel, W., 2013. Geologische Übersichtskarte der Republik Österreich 1:1 500 000 (ohne Quartär). In: Schuster, R., Daurer, A., Krenmayr, H.-G., Linner, M., Mandl, G.W., Pestal, G. & Reitner, J.M. (2013), *Rocky Austria – Geologie von Österreich – kurz und bunt*. Geologische Bundesanstalt, Vienna, 80pp.
- Shinn, E.A., Lloyd, R.M., Ginsburg, R.N., 1969. Anatomy of a modern carbonate tidal-flat, Andros Island, Bahamas. *Journal of Sedimentary Petrology*, 39, 1202–1228. <https://doi.org/10.1306/74D71DCF-2B21-11D7-8648000102C1865D>
- Spalluto, L., Moretti, M., Festa, V., Tropeano, M., 2007. Seismically-induced slumps in Lower-Maastrichtian peritidal carbonates of the Apulian Platform (southern Italy). *Sedimentary Geology*, 196, 81–98. <https://doi.org/10.1016/j.sedgeo.2006.06.009>
- Spengler, E., 1918. Die Gebirgsgruppen des Plassen und Hallstätter Salzberges im Salzkammergut. *Jahrbuch der Geologischen Reichsanstalt*, 68, 1–190.
- Strauss, P., Granado, P., Muñoz, J.A., 2021. Subsidence analysis of salt tectonics-driven carbonate minibasins (Northern Calcareous Alps, Austria). *Basin Research*, 33, 968–990. <https://doi.org/10.1111/bre.12500>
- Strozyk, F., van Gent, H., Urai, J.L., Kukla, P.A., 2012. 3D seismic study of complex intra-salt deformation: An example from the Upper Permian Zechstein 3 stringer, western Dutch offshore. In: Alsop, G.I., Archer, S.G., Hartley, A.J., Grant, N.T., Hodgkinson, R. (eds.), *Salt Tectonics, Sediments and Prospectivity*. Geological Society, London, Special Publications. Geological Society, London, 363, 489–501. <https://doi.org/10.1144/SP363.23>
- Suzuki, H., Gawlick, H.-J., 2009. Jurassic radiolarians from cherty limestones below the Hallstatt salt mine (Northern Calcareous Alps, Austria). *Neues Jahrbuch für Geologie und Paläontologie-Abhandlungen*, 251, 155–197. <https://doi.org/10.1127/0077-7749/2009/0251-0155>
- Tollmann, A., 1976. Analyse des Klassischen Nordalpinen Mesozoikums. Franz Deuticke, Vienna, 576 pp.
- Tollmann, A., 1985. *Geologie von Österreich: Band II Außerzentralalpiner Anteil*. Franz Deuticke, Vienna, 710 pp.
- Vendeville, B.C., Jackson, M.P.A., 1992. The fall of diapirs during thin-skinned extension. *Marine and Petroleum Geology*, 9, 354–371. [https://doi.org/10.1016/0264-8172\(92\)90048-J](https://doi.org/10.1016/0264-8172(92)90048-J)
- Vidal-Royo, O., Rowan, M.G., Ferrer, O., Fischer, M.P., Fiduk, C.J., Canova, D.P., Hearon IV, T.E., Giles, K.A., 2021. The transition from salt diapir to weld and thrust: Examples from the Northern Flinders Ranges in South Australia. *Basin Research*, 33, 2675–2705. <https://doi.org/10.1111/bre.12579>
- Wagreich, M., Decker, K., 2001. Sedimentary tectonics and subsidence modelling of the type Upper Cretaceous Gosau basin (Northern Calcareous Alps, Austria). *International Journal of Earth Sciences*, 90, 714–726. <https://doi.org/10.1007/s005310000181>

Received: 24.3.2022

Accepted: 10.9.2022

Editorial Handling: Hugo Ortner

# ZOBODAT - [www.zobodat.at](http://www.zobodat.at)

Zoologisch-Botanische Datenbank/Zoological-Botanical Database

Digitale Literatur/Digital Literature

Zeitschrift/Journal: [Austrian Journal of Earth Sciences](#)

Jahr/Year: 2022

Band/Volume: [115](#)

Autor(en)/Author(s): Fernandez Oscar, Grasemann Bernhard, Sanders Diethard

Artikel/Article: [Deformation of the Dachstein Limestone in the Dachstein thrust sheet \(Eastern Alps, Austria\) 167-190](#)